AD-A093 429 GENERAL DYNAMICS GROTON CT ELECTRIC BOAT DIV F/G 13/10
ANALYTICAL MODELLING OF STRUCTURAL DISTORTION IN SHIP STRUCTURE--ETC(U)
NOV 80 M BARTEK, F KOCON, N D OSELLA N00014-76-C-0808
UNCLASSIFIED U443-80-058 NL

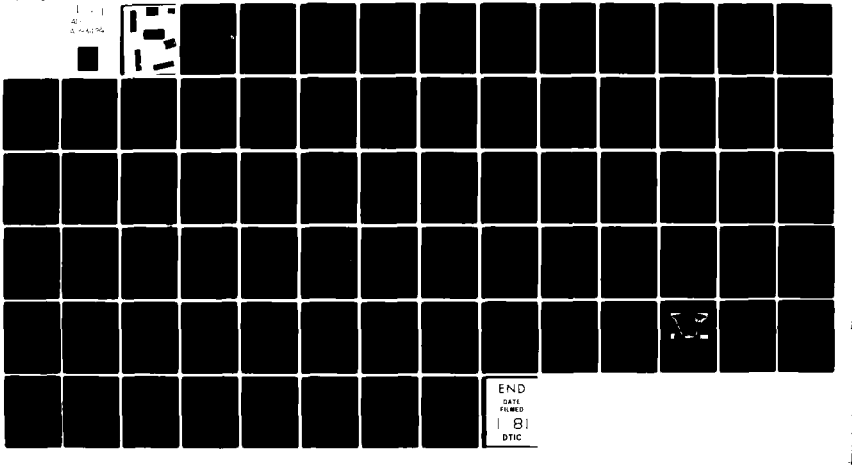

END
DATE FILMED
1 81
DTIC

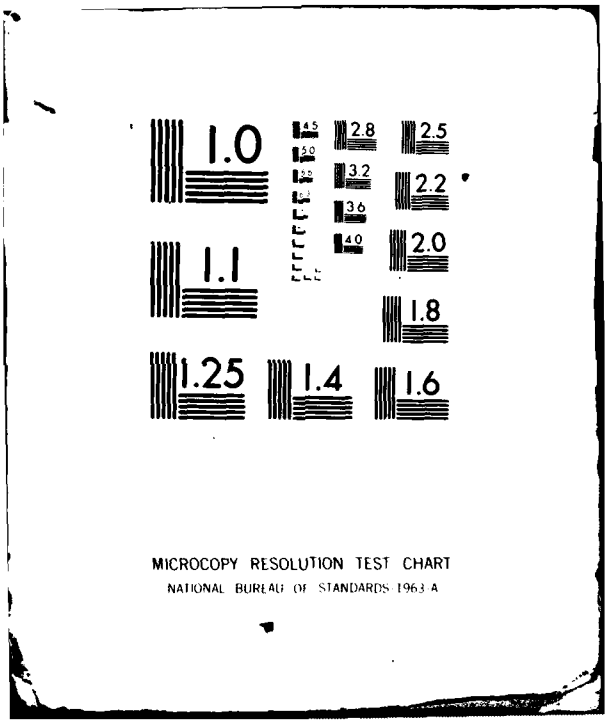
1.0
1.1
1.25
1.4
1.6
1.8
2.0
2.2
2.5
2.8
3.2
3.6
4.0
4.5
5.0
MICROCOPY RESOLUTION TEST CHART
NATIONAL BUREAU OF STANDARDS 1963 A

(9) Technical rept. Jul 78-Jul 80 (12)

Technical Report No. 3
Office of Naval Research
Contract No. N00014-76-C-0808

(15)

(11) Nov 80

ANALYTICAL MODELLING OF STRUCTURAL DISTORTION IN SHIP STRUCTURES PRODUCED BY WELDING

by

(10) M. Bartek
F. Kocon
N. D. Osella

Systems Technology Department
Electric Boat Division
GENERAL DYNAMICS
Groton, Connecticut

Prepared for
Office of Naval Research
Metallurgy Program
Arlington, Virginia 22217

(14) U443-80-058, TR-3
November 1980

1231:0 (14)

TABLE OF CONTENTS

I. BACKGROUND AND OBJECTIVES

In July 1976, a contract was awarded by the Office of Naval Research to Electric Boat Division in the area of computer analysis of welded ship structures. The overall objective of this research was to apply and further develop where necessary the technology for predicting distortion of submarine structure due to welding. The underlying motivation in providing this technology is that it can be used in design and construction of submarines to help determine the most cost effective weld joint designs and welding procedures. The specific objectives of the initial contract were:

1) implementation of MIT finite element computer programs for prediction of temperatures, residual stresses, and distortion due to welding;

2) evaluation of MIT computer programs on a fusion weld of two plates and comparison with results obtained by MARC-CDC finite element program;

3) analysis of a butt welded unrestrained plate with MIT computer codes and comparison with test results.

The results of that study are documented in Reference 1. In June 1977, a contract modification extended the scope of the initial contract to the following major technical objectives:

1) transient thermoplastic analysis of a butt welded unrestrained plate using the Electric Boat Division modified NONSAP finite element computer code,

2) further development and application of the Shrinkage Force Method (SFM) to welding analysis including investigation of weld bead sequencing, non-symmetry in the weld groove and remelt effects. The SFM is a simplified analytical approach for predicting weld distortion.

The results of that study are documented in Reference 2.

A second contract modification was awarded in September 1978 to apply the developed analytical methods to circumferential butt welding. An experiment conducted at the Massachusetts Institute of Technology on an HY-130 cylinder butt weld (Reference 3) was chosen as the test problem for further evaluation of the transient thermoplastic analysis and Shrinkage Force Method developed under the initial contract and first modification. In addition application of the Shrinkage Force Method to multipass, circumferential welding of submarine HY-80 ring stiffened cylinder sections was also included in the workscope. The analytical approach employed in this latter task was developed under Electric Boat Division IRAD Task 573. It utilizes a layered shell approximation to simulate the weld build-up.

The results of these latest studies are documented in this report.

II. THERMOMECHANICAL DISTORTION ANALYSIS OF MULTIPASS GIRTH WELDING IN AN HY-130 CYLINDER

The objective of this segment of the contract was to analytically predict weld distortion due to girth welding of an HY-130 cylinder and compare the results with available test data. The cylinder considered was the 18" diameter, HY-130 test sample (see Figure II-C-2) GMAW welded at the Massachusetts Institute of Technology and reported in Reference 3.

The approach to the mathematical modelling problem was as follows:

a. Analytically predict the transient temperature distribution during girth welding.

b. Analytically predict transient thermoplastic distortions using the above predicted transient temperatures.

c. In addition apply the Shrinkage Force Method to predict thermomechanical distortions.

Detailed discussions of the analyses and results are presented in the following sections.

II-A HEAT TRANSFER ANALYSIS

o Introduction

A heat transfer analysis was made using the TEMP computer program, in order to calculate the temperature transients required by the ensuing NONSAP structural analysis. This thermal transient program, which uses the finite element analysis technique, is based on the work described in Reference 4. The program was obtained in 1978 during a computer workshop at Union College in Schenectady, New York.

The program can be used on either one or two dimensional plane or axisymmetric bodies. Boundary conditions of convection, radiation, heat flux or nodal temperature may be specified, and all boundary conditions can be functions of time.

Five different materials may be used with the associated thermal properties considered to be quadratic functions of temperature about a specified reference temperature. The proper selection of coefficients and reference temperature can yield either a linear property variation with temperature or a constant property value.

The utilization of the TEMP computer program also allowed the use of the same model elemental break-up as used by NONSAP. Thus, the required nodal temperatures were computed directly, and the need for spatial interpolation was eliminated.

o Thermal Model and Analysis

The analytical model, excluding the elemental break-up, is shown in Figure II-A-1. The model is a two dimensional, axi-symmetric representation of the HY-130 cylinder. In this case the TEMP program uses elemental depths (lengths in the circumferential direction) associated with an angle of one radian. This yields element depths of approximately nine inches. The weld region is represented as three weld layers rather than the actual six bead lay-up which is somewhat questionable as to its thermal modelling accuracy, since each layer is composed of several beads which are actually deposited at different times. (See Figure II-C-10.) The elements and nodes associated with the three weld layers are shown in Figure II-B-2. The first weld layer is composed of elements 6001 through 6009, the second weld layer is composed of elements 6010 through 6015, and the third weld layer is composed of elements 6016 through 6021. Each weld layer deposition was modelled as an instantaneous addition of the weld metal at its vaporization temperature of $5000^{o}F$ at time equal to zero resulting in a separate thermal

analysis for each of the three weld layer depositions. It was also assumed that the base metal and any previously deposited weld layers were preheated to a temperature of 200°F at time equal to zero. The resulting initial condition for each temperature transient calculation was that all nodes of the weld layer being deposited were at a temperature of 5000°F, and all other nodes of the structure were at a temperature of 200°F. As the transient progressed the deposited weld layer, which was assumed to have the same thermal properties as HY-130, was cooled by conduction to the rest of the structure since it was assumed that the convective and radiative heat losses were negligible as indicated by the insulated surfaces on Figure II-A-1.

The heat addition approach used above differs from the "ramp heat flux" heat addition approach previously used for flat plate welding thermal analysis (Reference 1). The ramp approach assumes an applied heat flux which starts at a value of zero at zero time, increases to a prescribed value at a specified time, continues at a constant value for a given period of time, then decreases to zero at a certain time. It was felt that the ramp heat addition approach would not offer a good

representation of the actual heat input for this case, since the ramp would have to extend over the first 45 seconds of the thermal transient.

It was determined that the total heat released by the weld metal during a cooldown from 5000°F to 200°F would be 939 Btu per pound. Since the latent heat of fusion of 117 Btu per pound would be a small portion of the total (approximately 12%), it was neglected in order to simplify the analysis.

The thermal properties for HY-130 steel are presented in Table II-A-1. The following method was used to account for the thermal property variations, since the variations do not lend themselves to either the quadratic or linear representations of the TEMP computer program. The structure was divided into two sections; namely, a large low temperature (less than or equal to 400°F) section, and a small high temperature (greater than 400°F) section. The two sections were composed of different materials with different constant values for their thermal properties. The properties for each section were evaluated by taking an integrated average over the appropriate temperature range.

o Results

Typical predicted temperature transients for the first, second and third weld layer depositions for four nodal points are presented in Figures II-A-2 through II-A-4. The nodal point locations were selected such that the predictions for the first weld layer deposition could be compared to the experimental data of Reference 3. In Reference 3, experimental data is presented for the first weld pass only. It is unfortunate that experimental temperature data is not available for the other weld passes also. These comparisons are presented in Figures II-A-5 through II-A-8. As indicated by the figures, the predicted temperatures for the first weld layer deposition are substantially lower than the experimental values. It is felt that this discrepancy could be due to the use of inaccurate low values of specific heat capacity for the liquid metal weld layer at early times of the predicted transient. A substantially higher value would yield a higher temperature difference driving force for conduction, as well as more energy available for base metal heat-up.

T	68	200	400	600	800	1000	1200	1400	1600	1660	1800	2000	2200	2400	2600	2800
ρ	.2839	.2831	.2818	.2800	.2789	.2775	.2759	.2750	.2747	.2747	.2747	.2747	.2747	.2747	.2747	.2747
C	19.4	20.4	21.5	21.79	21.15	19.45	17.05	15.0	13.35	13.1	14.0	15.0	16.0	16.65	17.0	17.0
K	.1065	.11	.118	.126	.1355	.148	.168	.197	.255	.293	.18	.1575	.1575	.1575	.1575	.18

NOMENCLATURE

T = Temperature (^{o}F)

ρ = Density (Lb_m/in^3)

C = Thermal Conductivity (BTU/HR FT ^{o}F)

K = Specific Heat (BTU/Lb_m ^{o}F)

SUMMARY OF PHYSICAL PROPERTIES FOR HY-130 STEEL

TABLE II-A-1

Data obtained from Steven S. Chiu, DTNSRDC, Code 1720.1 Bethesda, Maryland - Source MIT

THERMAL ANALYTICAL MODEL

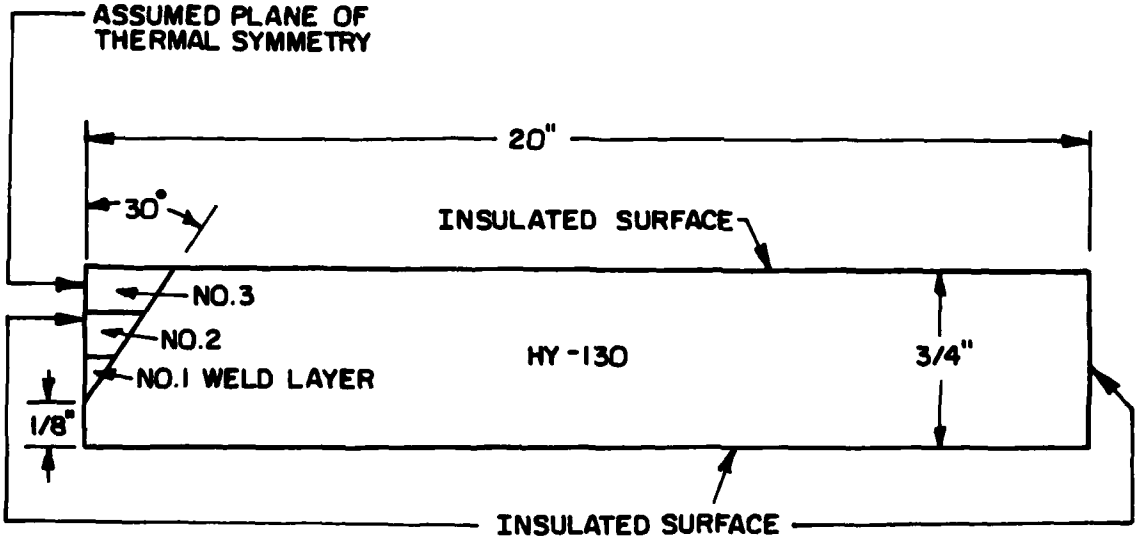

FIGURE II-A-1

PREDICTED TEMPERATURE TRANSIENTS FOR POINTS LOCATED ON OUTER SURFACE OF CYLINDER FOR FIRST WELD LAYER DEPOSITION

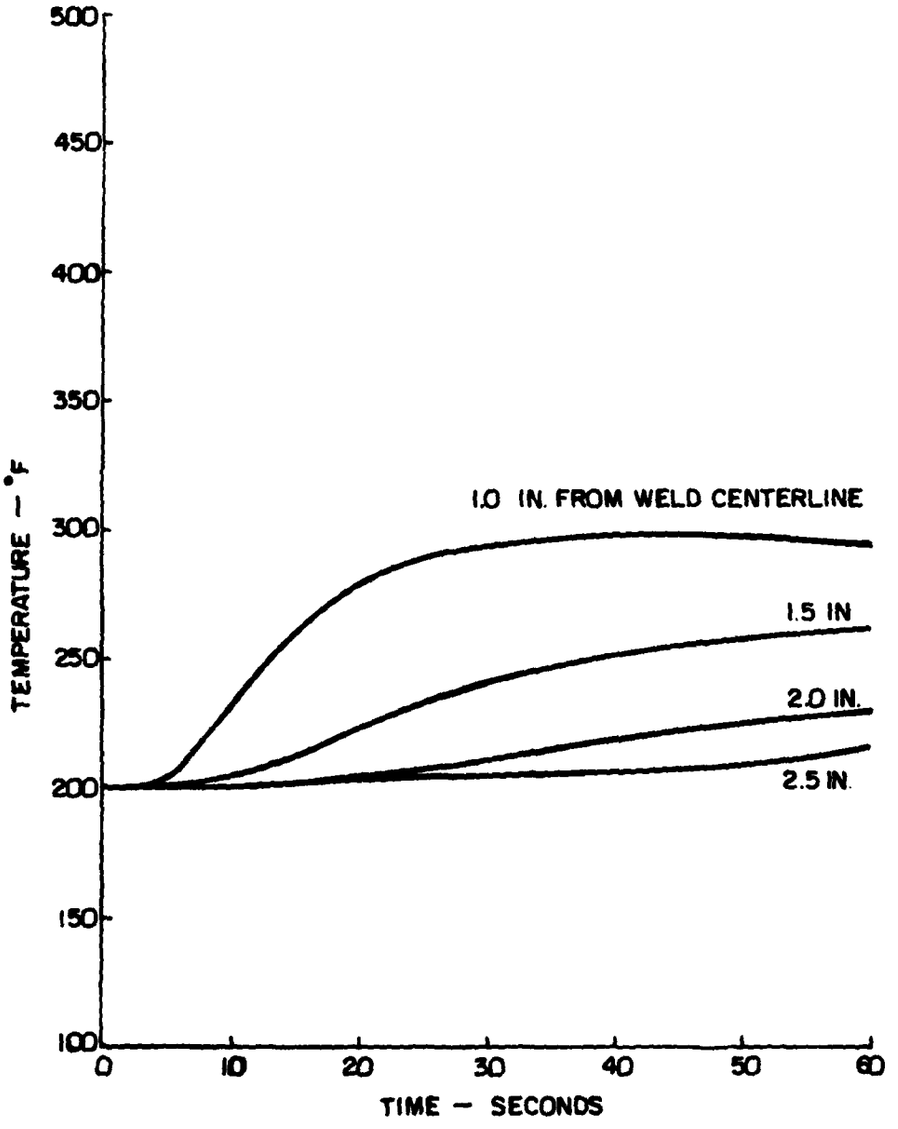

FIGURE II-A-2

PREDICTED TEMPERATURE TRANSIENTS FOR POINTS LOCATED ON OUTER SURFACE OF CYLINDER FOR SECOND WELD LAYER DEPOSITION

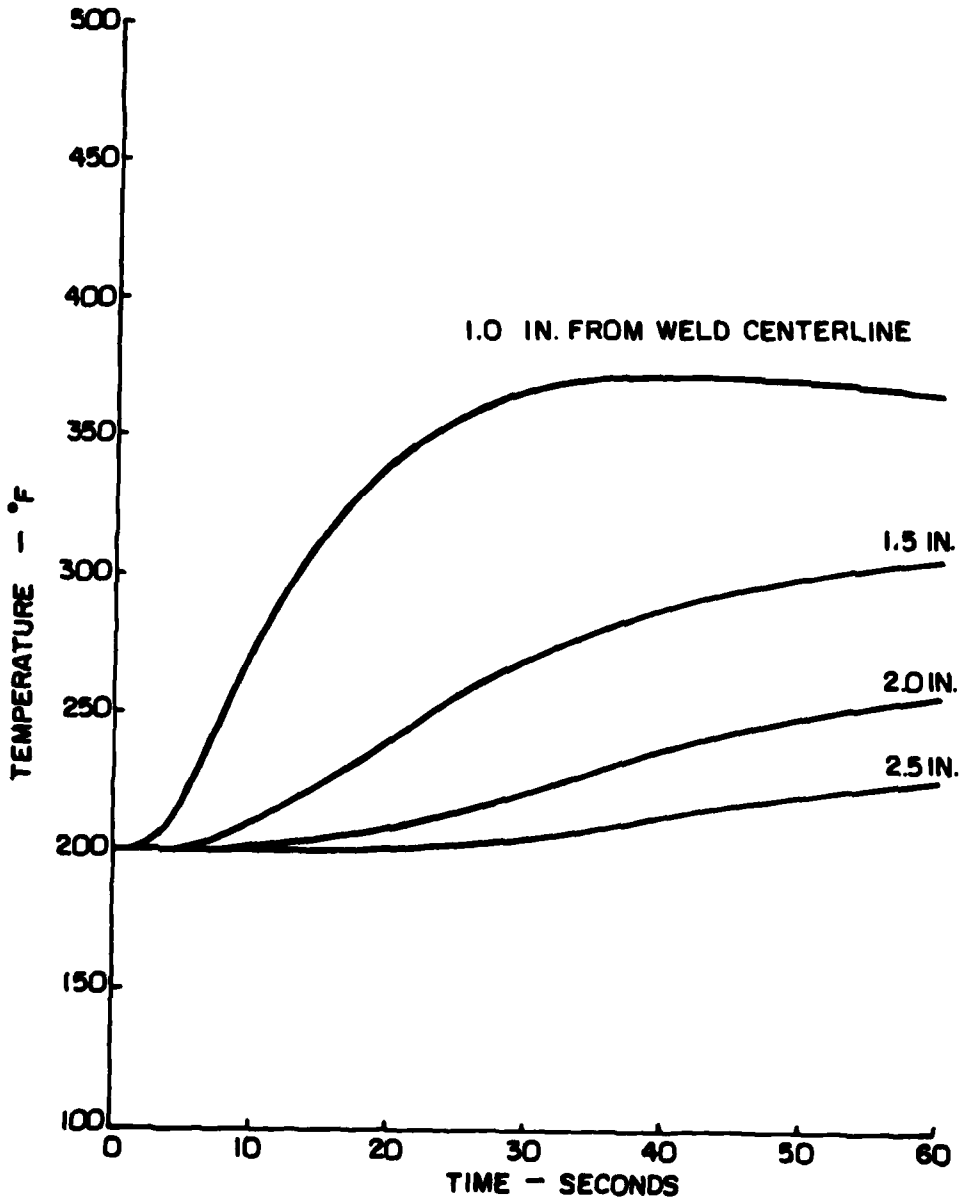

FIGURE II-A-3

PREDICTED TEMPERATURE TRANSIENTS FOR POINTS LOCATED ON OUTER SURFACE OF CYLINDER FOR THIRD WELD LAYER DEPOSITION

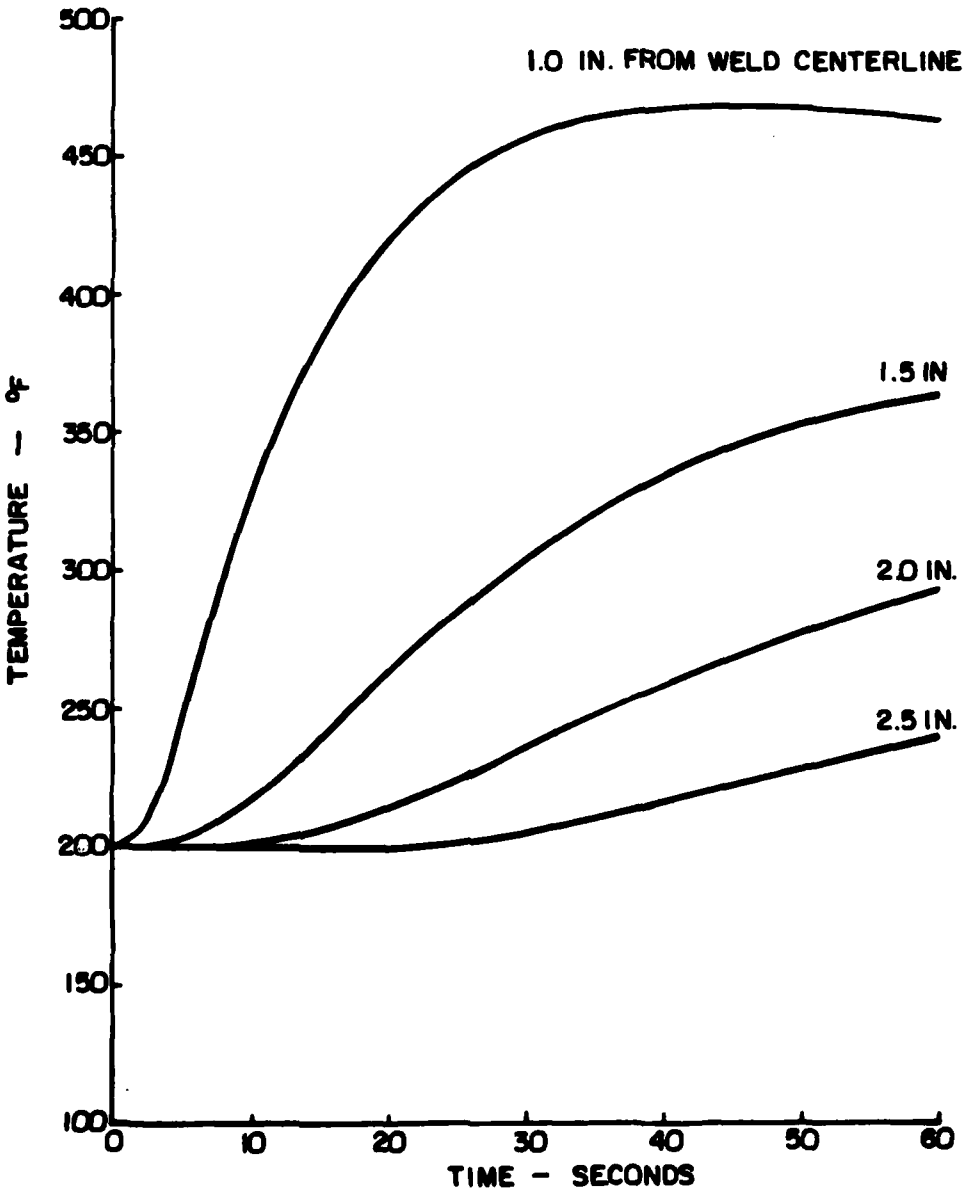

FIGURE II-A-4

COMPARISON OF EXPERIMENTAL AND PREDICTED TEMPERATURE TRANSIENT AT A POINT LOCATED 1.0 IN. FROM WELD CENTERLINE ON OUTER SURFACE OF CYLINDER

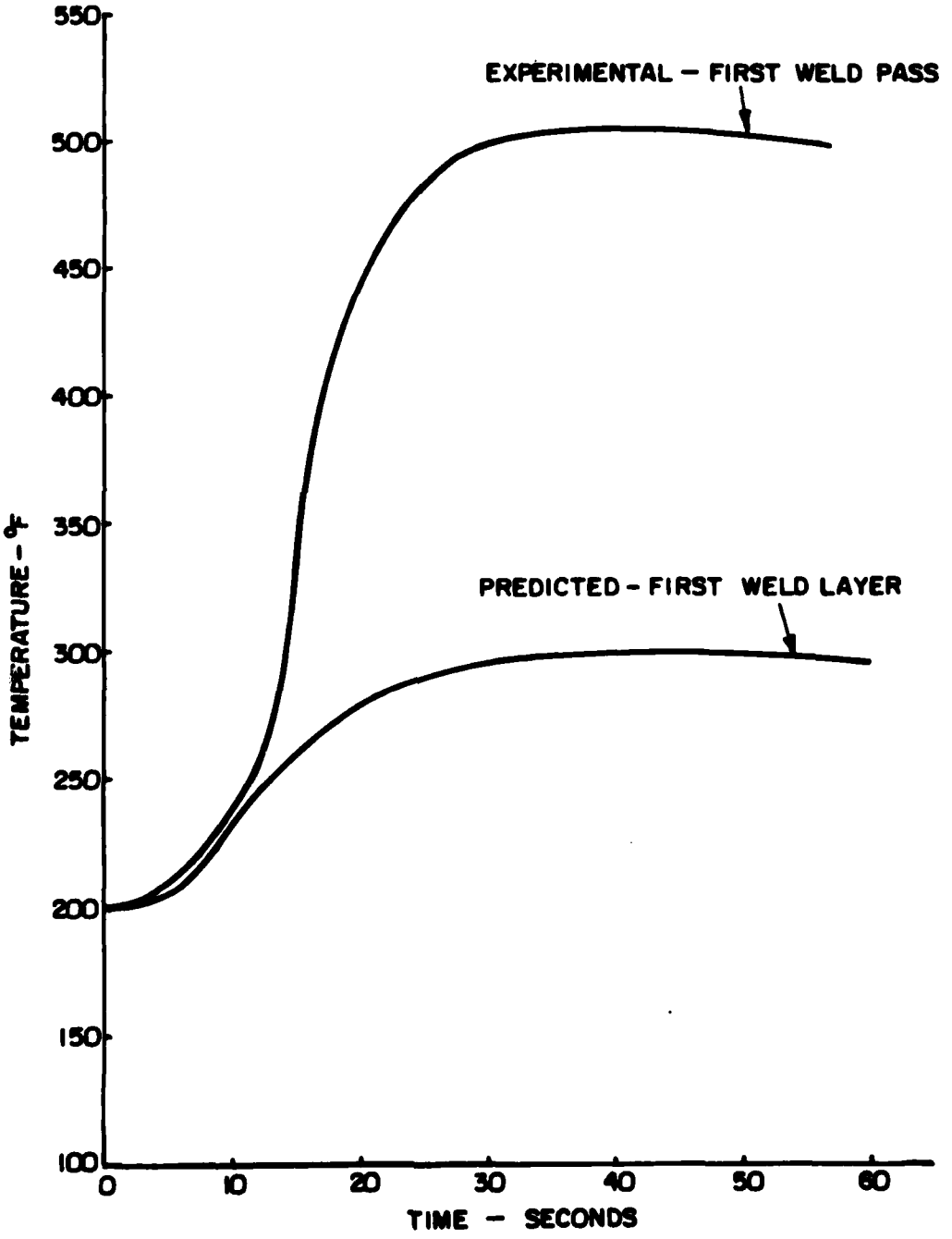

FIGURE II-A-5

COMPARISON OF EXPERIMENTAL AND PREDICTED TEMPERATURE TRANSIENT AT A POINT LOCATED 1.5 IN. FROM WELD CENTERLINE ON OUTER SURFACE OF CYLINDER

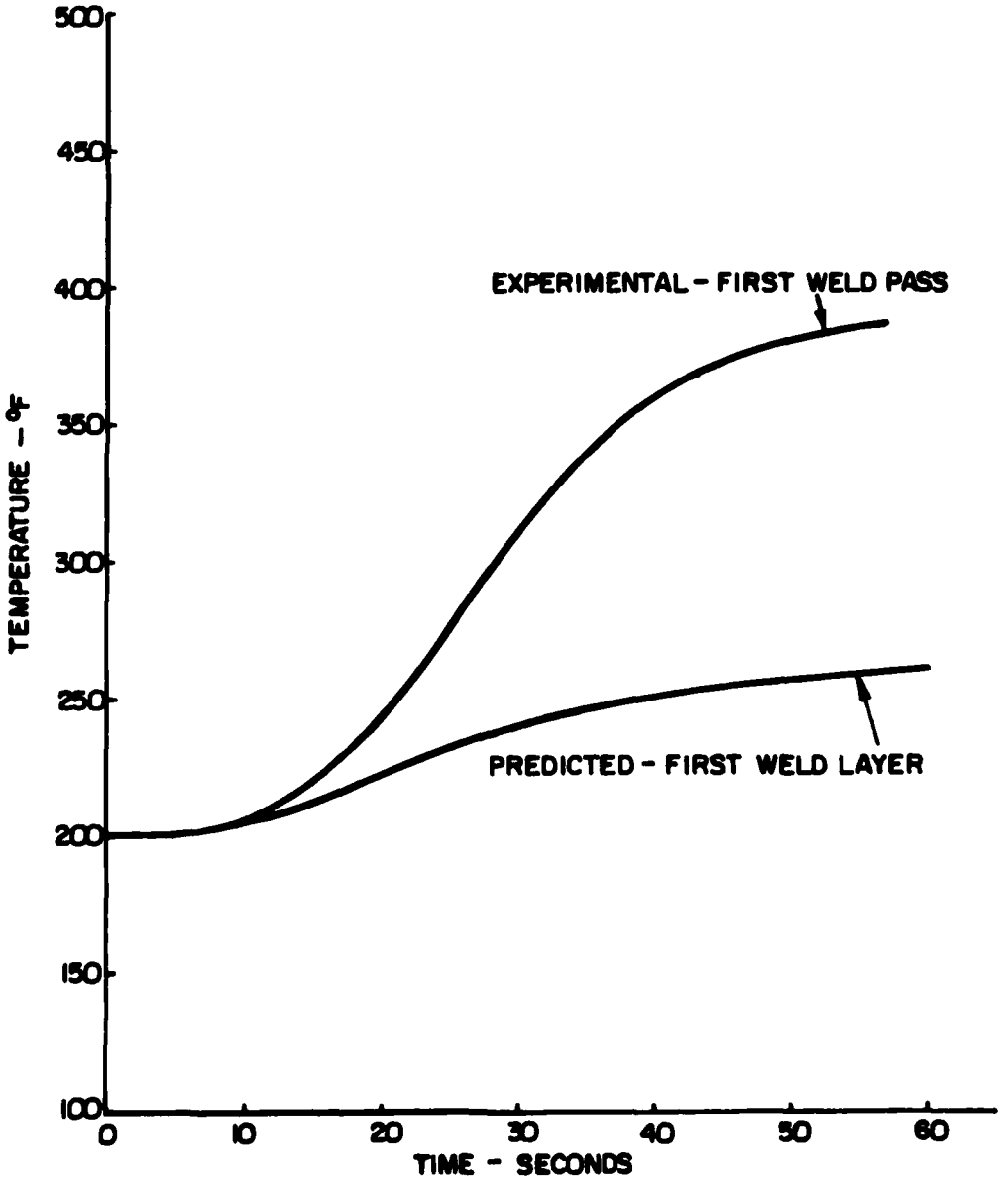

FIGURE II - A - 6

COMPARISON OF EXPERIMENTAL AND PREDICTED TEMPERATURE TRANSIENT AT A POINT LOCATED 2.0 IN. FROM WELD CENTERLINE ON OUTER SURFACE OF CYLINDER

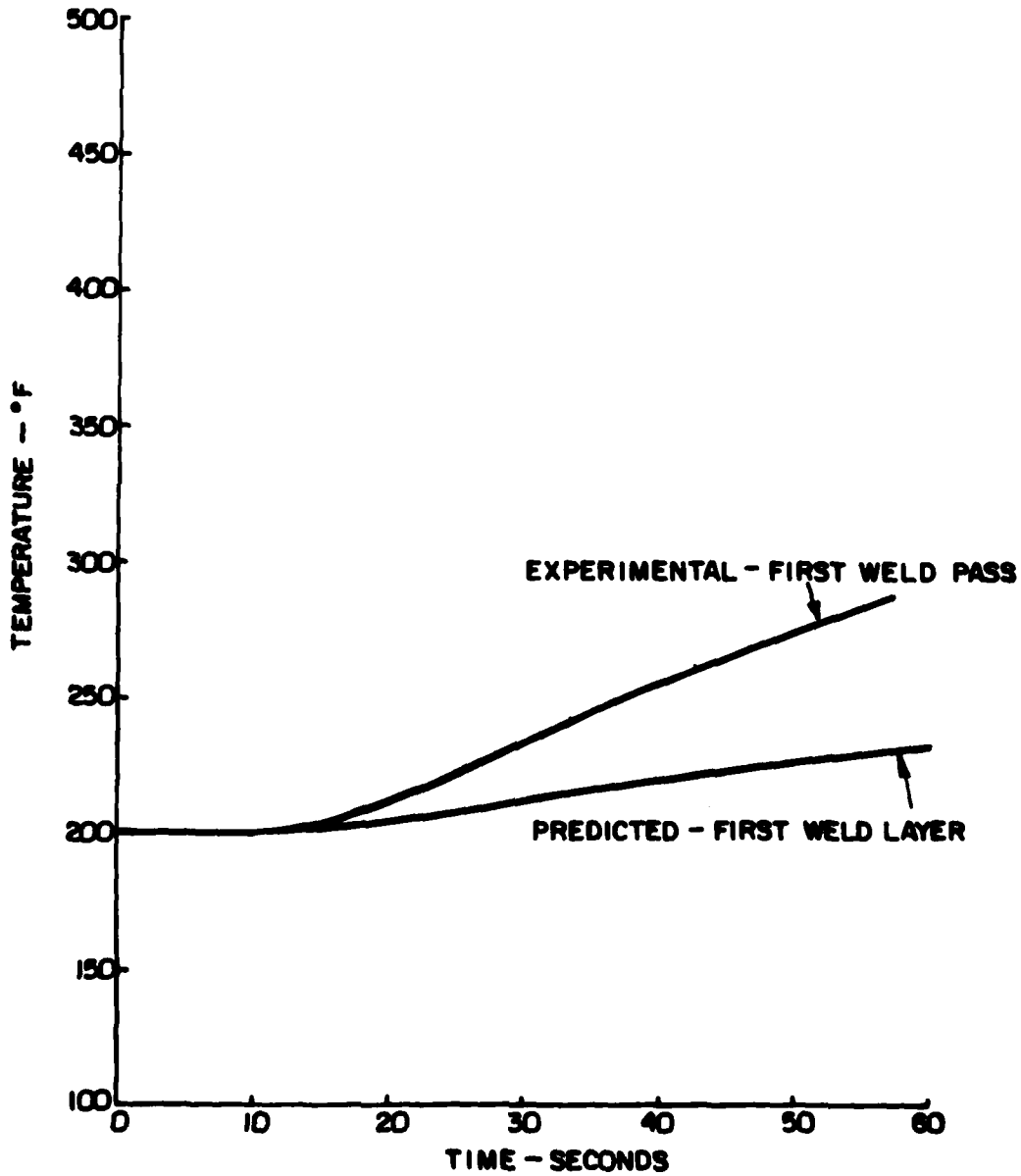

FIGURE II-A-7

COMPARISON OF EXPERIMENTAL AND PREDICTED TEMPERATURE TRANSIENT AT A POINT LOCATED 2.5 IN. FROM WELD CENTERLINE ON OUTER SURFACE OF CYLINDER

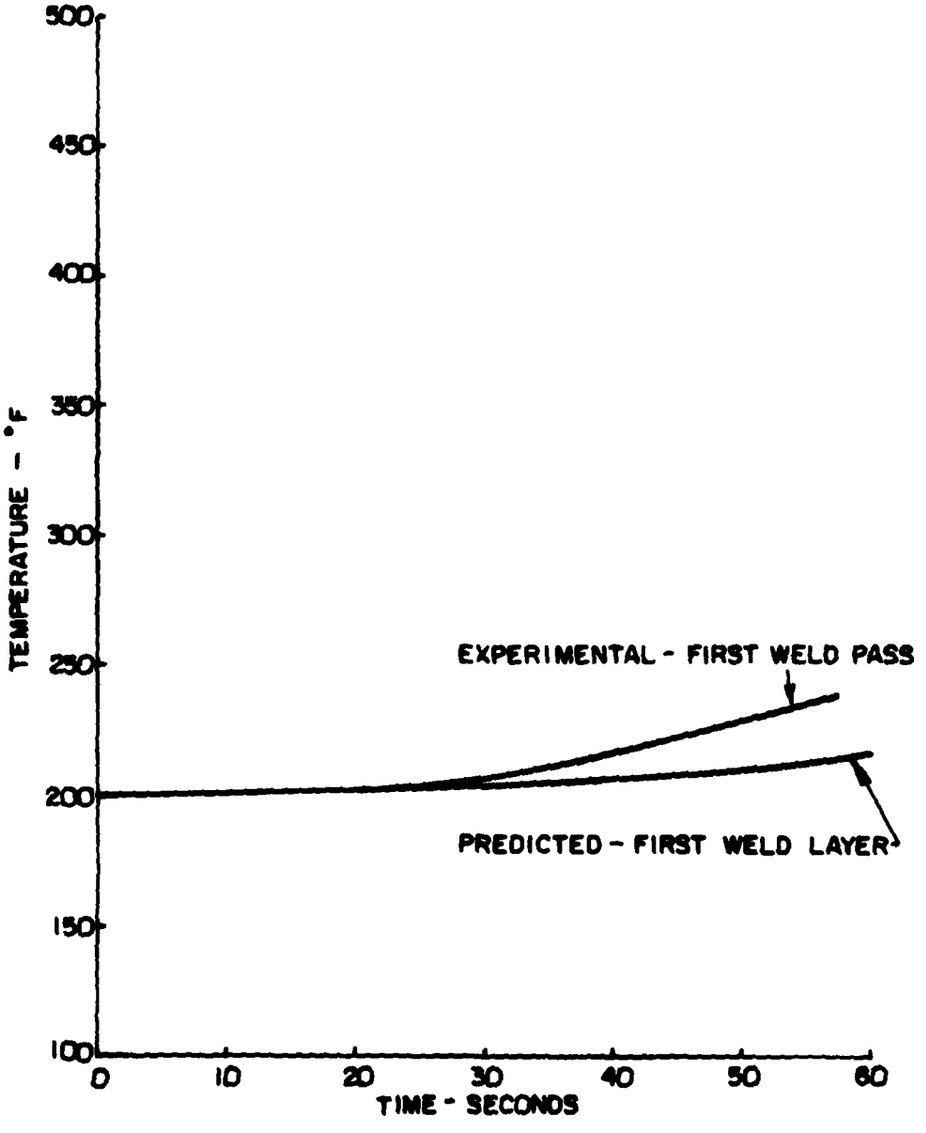

FIGURE II-A-8

II-B THERMOPLASTIC ANALYSIS (USING THE NONSAP COMPUTER PROGRAM)

o Introduction

In 1977 the NONSAP finite element program was modified to perform thermoplastic analysis with temperature dependent material properties. Additional modifications were made in 1978 to assist in the analysis of weld distortion problems. Specifically, a "birth" and "death" option was added for two dimensional finite elements that represent the weld deposit. At specified times during the analysis, the elements in the weld groove region may be activated (achieve strength from cooldown) or deactivated (melt). This added feature to the program greatly assists in the modelling of the weld region.

In 1979 the modified NONSAP program was applied to the HY-130 cylinder girth weld reported in Reference 3. The transient temperature distributions used in this analysis were calculated via the TEMP computer code as reported above in Section II-A.

o Analysis Methods

Figure II-B-1 shows the overall NONSAP finite element model used for the thermoplastic analysis. Figure II-B-2 shows the model of the weld groove region which is a three layer representation of the six weld beads used in the actual cylinder welding. Figures II-B-3 thru II-B-7 show the remainder of the model elements. The model employed symmetric boundary conditions in the weld groove region and free movement at the opposite end of the cylinder. The "+y" direction of the local coordinate system was in the radial direction and "+z" ran along the length of the shell.

Four-noded isoparametric, quadrilateral, plain-strain finite elements, with a 2x2 Gaussian integration scheme, were utilized in the analysis. The elements were reduced to triangular shape where necessary, to represent the geometry and to make transitions from large element size to small element size as the weld region is approached.

From the transient heat transfer analysis, a file of nodal temperature distributions as a function of time were generated to simulate the heatup-cooldown cycle caused by individual deposition of the three weld layers. The temperature dependency of the material properties used in this analysis are plotted in Figure II-C-1.

The math model used for the heat transfer analysis was identical to the NONSAP analysis math model. This allowed a sequence of temperature distributions from time = 0.0 seconds to time = 60.0 seconds. The maximum temperature change between any two nodes in going from time (i) to time (i + 1) ranged from 0.0 to 4800^{o}F.

From these nodal temperatures, the temperature at the four Gauss points in each finite element is calculated in NONSAP. The tangent stiffness is then calculated using the material properties associated with the current temperature and stresses at the Gauss points. The increment of thermal load in going from time (i) to time (i + 1) is applied to obtain the increment in nodal deflections and the associated incremental stresses at the Gauss points assuming elastic behavior. Then, the total stress at each Gauss point is compared to the Von Mises yield surface at the current temperature to determine whether the increment in stress calculated elastically is admissable or whether the yield surface has been exceeded. If the yield surface has been exceeded, the stresses are adjusted to be consistent with the specified plastic behavior model.

Equilibrium iterations in the NONSAP program are performed until the displacement has converged to within a 0.005 error tolerance. Within each of these iterations, the stresses are updated, checked against the yield surface, and corrected if necessary.

o Analysis Results

The initial approach was to analyze each of the weld layers with a successive series of heatup-cooldown cycles introducing weld layers 1 thru 3 at the appropriate times. The approach had to be abandoned during the cooldown of weld layer 1 (elements 6001 to 6009), when unresolvable convergence difficulties developed. A considerable effort was made to obtain convergence of the solution, however no solution strategy was found to accomplish this. When the solution was continued to the next time step, the displacement solution blew up. The following is a possible reason the analysis would not converge:

The nodal temperature at the four Gauss points in each finite element is calculated. The tangent stiffness of the element is then calculated using the material properties associated with the current temperature. The weld region which has small elements experiences large stiffness changes due to the temperature transients of the heatup and cooldown cycles. The remaining portion of the model which has relatively larger elements maintains an average stiffness due to the smaller changes in temperature. The combination of the weld region experiencing drastic changes in stiffness and the larger elements having a relatively constant stiffness may be causing an ill-conditioned matrix.

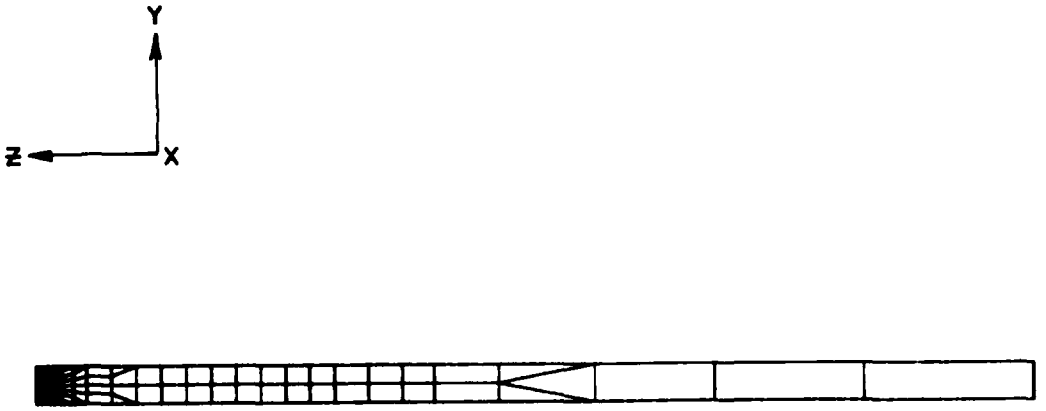

THERMOPLASTIC MATH MODEL

FIGURE II - B - 1

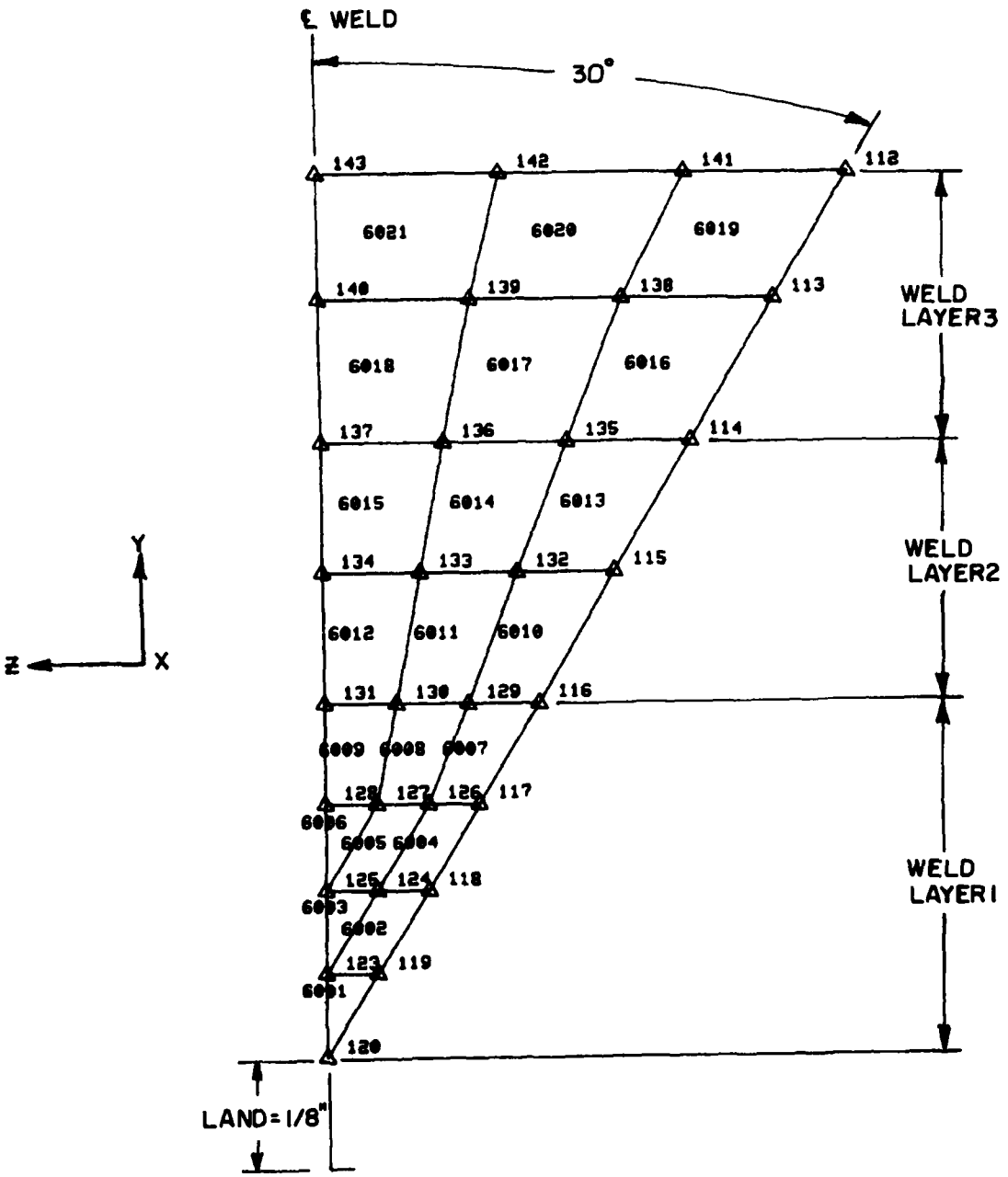

THERMOPLASTIC MATH MODEL
WELD LAYER ELEMENTS 6001-6021

FIGURE II-B-2

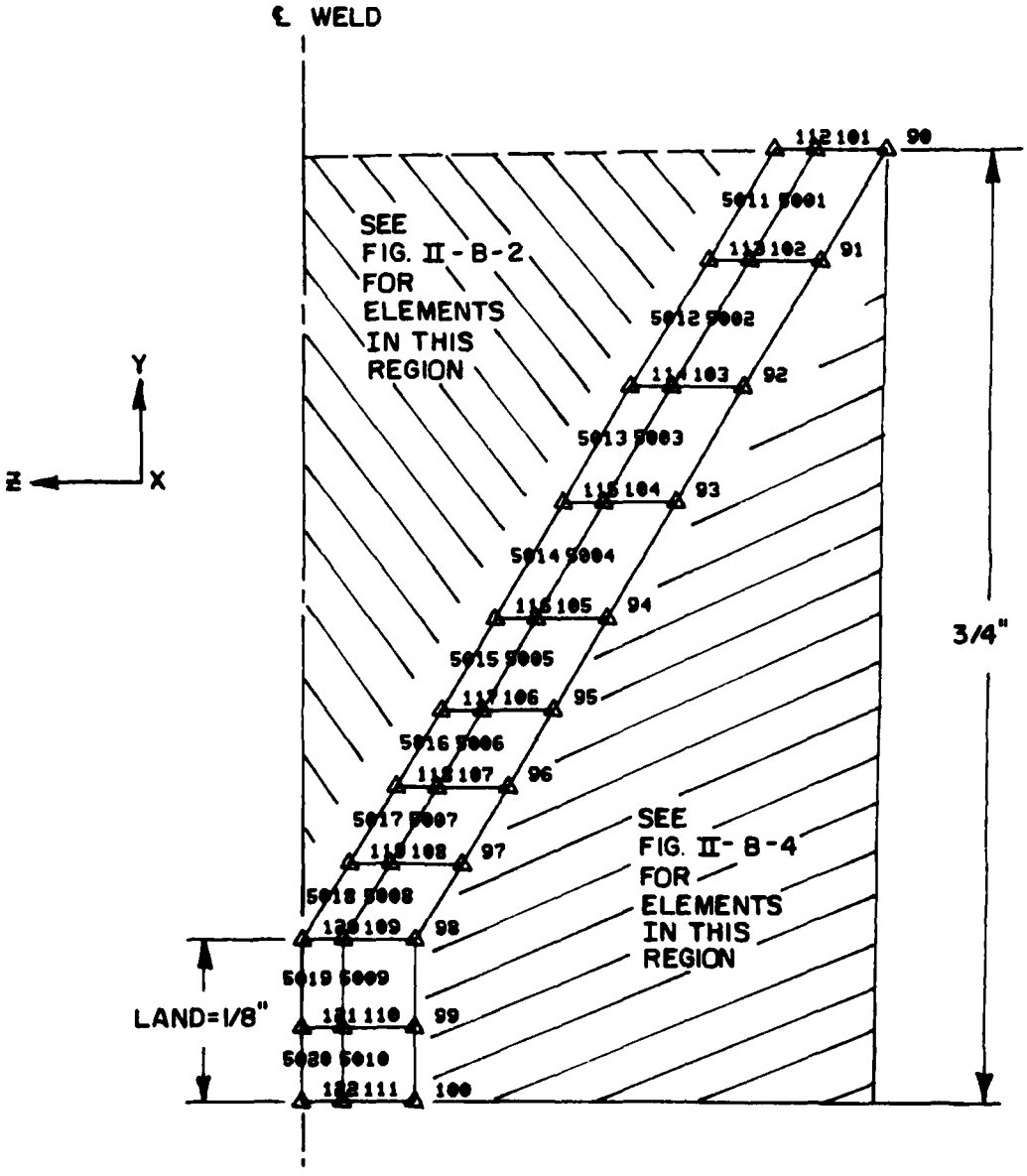

THERMOPLASTIC MATH MODEL
ELEMENTS 5001-5020

FIGURE II-B-3

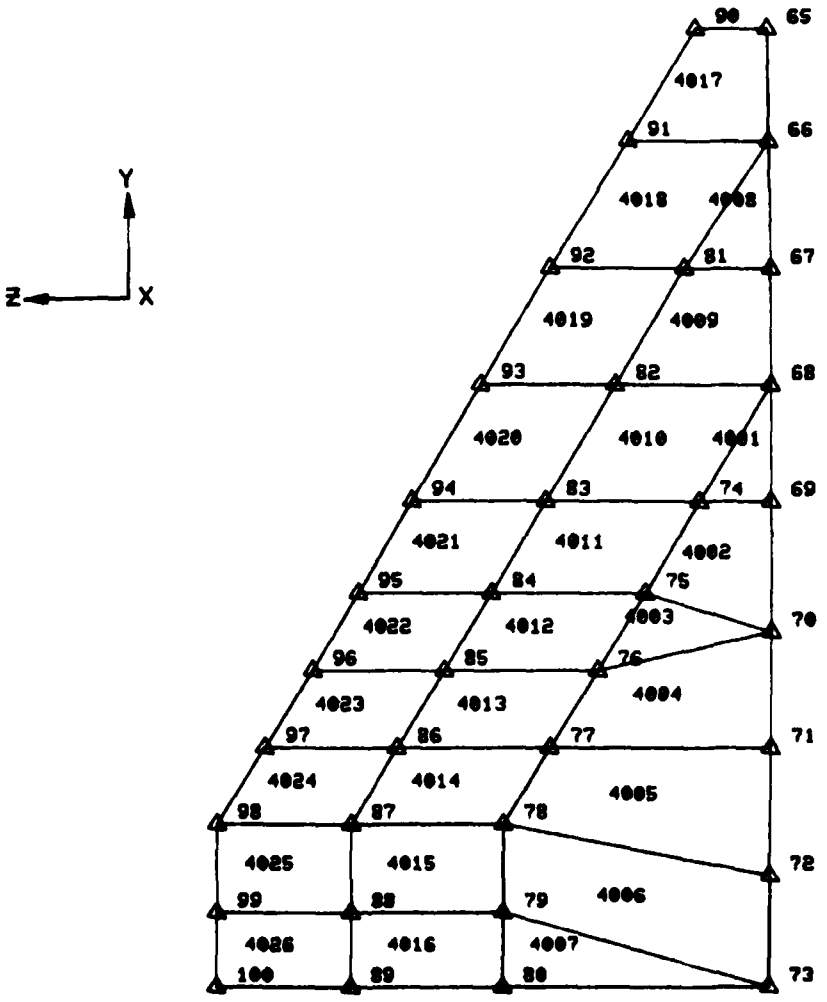

THERMOPLASTIC MATH MODEL
ELEMENTS 4001-4026

FIGURE II-B-4

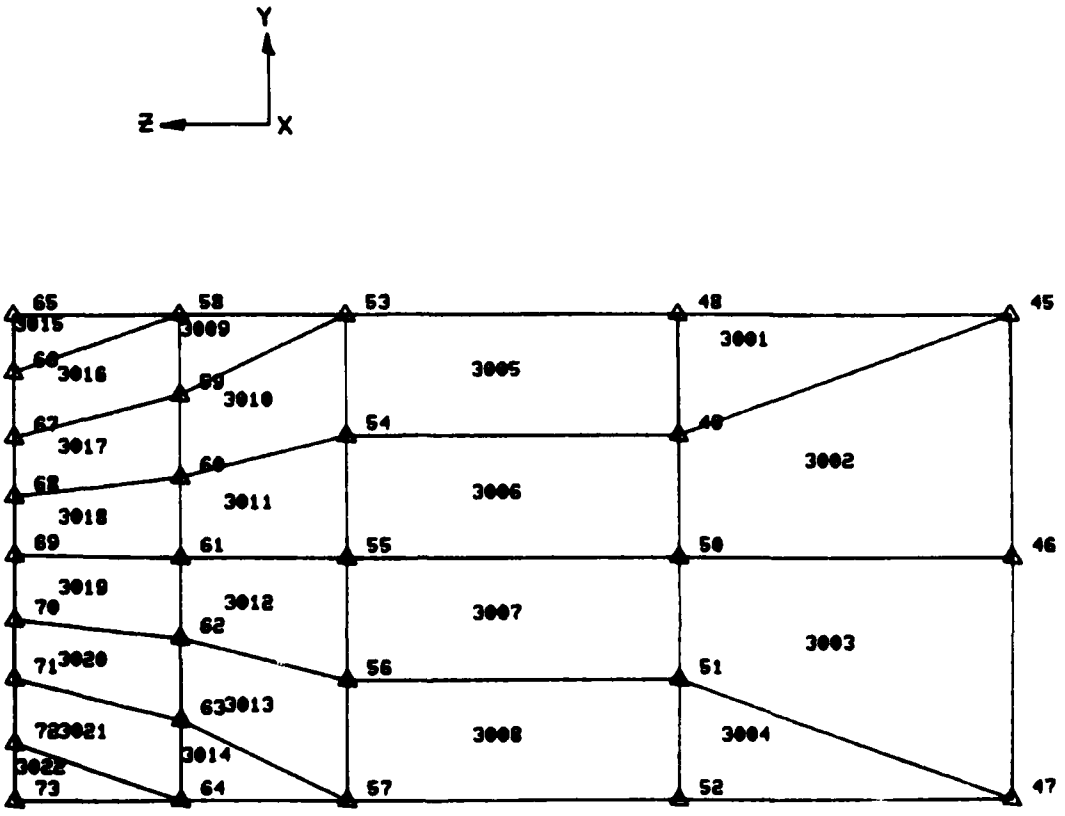

THERMOPLASTIC MATH MODEL
ELEMENTS 3001-3022

FIGURE II-B-5

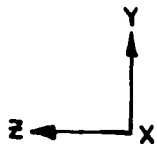

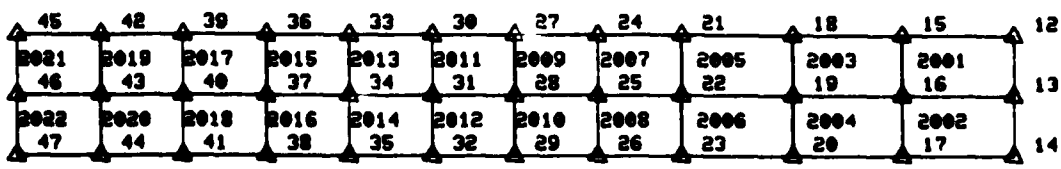

THERMOPLASTIC MATH MODEL
ELEMENTS 2001 - 2022

FIGURE II - B - 6

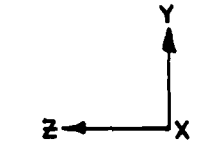

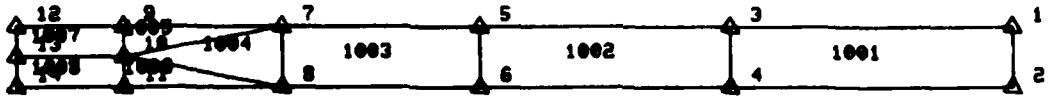

THERMOPLASTIC MATH MODEL
ELEMENTS 1001 - 1007

FIGURE II - B - 7

II-C. SHRINKAGE FORCE METHOD

o Introduction

This weld distortion prediction technique is based upon the assumption that the shrinkage forces developed in each weld layer during thermal cooldown are the major contributors to distortion. In the application of the method, the geometry of each weld layer along with the appropriate temperature changes (ΔT) for the cooldown of the weld metal must be known. In its simplest form the linear coefficient of thermal expansion (α_T) and Young's modulus (E) are used to calculate the linear contraction force layer by layer. This is applied to the workpiece in a series of numerical solutions for distortions. The procedure can approximately account for the variation with temperature of material properties (E and α in the elastic case) by simply using an integrated average over the cooldown temperature range. The primary feature of the SFM method is the elimination of the need for an expensive time dependent nonlinear heat transfer analysis.

o Idealization of Material Properties

The material properties used in applying the Shrinkage Force Method of analysis to the NONSAP computer code are presented in Table II-C-1 and Figure II-C-1. NONSAP is limited to six (6) data points to define material properties as a function of temperature and assumes a linear relationship between the data points. A temperature of 2500^{O}F was used as the starting point for cooldown in the analysis since this point represents the temperature where the weld metal starts to achieve strength.

o Finite Element Model

The finite element model developed and used to predict distortion caused by multipass welding in the HY-130 cylinder is shown in Figure II-C-3. A twenty inch long segment of the eighteen inch diameter cylinder was modeled with a 60 degree included angle single vee outside weld prep with 1/8 inch land. The weld region consisted of a three layer representation of the six weld beads used to fill the joint shown in Figure II-C-2. A detailed breakup of the finite element model showing joint and element numbering is shown in Figures II-C-4 thru II-C-10. This model is a mirror

image of the one used in the previous section. The origin of the model was located at the weld centerline with positive "y" along the radial direction and position "z" along the length of the cylinder. Symmetry boundary conditions were applied at the weld centerline (0,0) while the opposite edge of the cylinder was free.

o Analytical Approach

Similar to the approach used in the previous section, the SFM idealized the cylinder as a two dimensional axisymmetric problem. The model employed two dimensional four noded isoparametric, quadrilateral, plain strain finite elements, with a 2x2 Gaussian integration scheme. The elements were reduced to triangular shapes where necessary to represent the geometry and for transition from large element size to small element size near the weld region.

The HY-130 material was assumed to have six different moduli (E = 1,2,3,...6) and thermal coefficients (α_T = 1,2,3,...6) in each layer analysis. Values for E, α_T, and ΔT are given in Table II-C-1 and shown in Figure II-C-1.

The distortion for each weld layer as it cools down is computed and displacements are simply accumulated layer by layer. The model reflects the changing geometry as each layer is added. Internal stresses are also accumulated throughout the analysis. When the weld elements are activated at T = 2500^{o}F, the internal stresses within the previously cooled material, which is then assumed to remelt, are set equal to zero (i.e. no strength is assumed), and the change in deflection is computed for this condition.

The deflections and internal stresses are accumulated for solidification and remelt cycles until the final deformed state is determined.

Equilibrium iterations are performed until the displacement solution has converged to within a 0.005 error tolerance. Within each iteration, the stresses are updated.

The approach used to analyze the HY-130 cylinders was as follows:

1)	Start heatup cycle for layer 1 at 200^{o}F (preheat temperature) for all joints in the model.	TIME=0.0
2)	Heat joints along the weld prep's edge to 2500^{o}F, to make them compatible with the layer 1 weld joints to be introduced.	TIME=1.0 to TIME=10.0

3) Activate layer 1 weld joints and elements of the model at a temperature of 2500°F. TIME =11.0

4) Cooldown layer 1 model from 2250°F to 200°F, preheat temperature. TIME =12.0 to TIME =20.0

5) Begin heatup cycle for layer 2. A problem was encountered at this point in re-starting the analysis for second layer heatup; (T = 500°F) due to no convergence at affected nodes. TIME =21.0

The solution to this problem was to go up in small temperature increments at first, until good convergence was reached. The following incremental runs were used to reach 500°F.

TIME	TEMP. AT AFFECTED NODES °F
20.2	225
20.4	250
20.6	300
20.8	400
21.0	500

Convergence was reached at time = 21.0, T = 500°F and saved.

Continued heatup for layer 2. TIME =22.0 TO TIME =29.0

6) Activate layer 2 weld elements and joints at $T = 2500^{\circ}F$. TIME=30.0

7) Start cooldown cycle for layer 2 from $2250^{\circ}F$ to $200^{\circ}F$. Again a problem was encountered due to no convergence. The solution to this was to let the temperature stay at $2500^{\circ}F$ for two analyses to achieve good convergence; then start dropping temperature with small ΔT's to $2250^{\circ}F$. The following runs were made: TIME=31.0

TIME	TEMP. AT AFFECTED NODES $^{\circ}F$
30.2	2500.0
30.4	2500.0
30.6	2475.0
30.8	2400.0
31.0	2250.0

Good convergence was achieved and the analysis proceeded through the cooldown cycle.

Continue cooldown to preheat temperature for all affected nodes. TIME=32.0 TO TIME=40.0

NOTE

Due to the convergence difficulties encountered in the heatup and cooldown cycles for layer two, interim analyses were made for layer three to avoid these problems again.

8)	Heatup for layer 3.	TIME=41.0 TO TIME=49.0
9)	Activate layer 3 weld joints and elements at T = 2500^{o}F.	TIME=50.0
10)	Cooldown cycle for layer 3.	TIME=51.0 TO TIME=60.0
11)	Analysis complete.	

o Analysis Results

Figure II-C-11 shows the cumulative radial distortion at the weld centerline versus the NONSAP run sequence number. The run sequence number corresponds to an applied material temperature (^{o}F) used in the NONSAP analysis. These are tabulated in Table II-C-2 along with the corresponding temperature and heatup or cooldown cycles for each layer. The distortion pattern for each layer is generally characterized by distortion relief during the heatup cycle and increasing distortion during the cooldown cycle.

Figure II-C-12 shows the layer by layer radial distortion along the length of the cylinder. As can be seen the greatest amount of distortion occurs within 2.0 inches from the weld centerline for each layer, and rapidly diminishes after that point. A final distortion prediction of -0.0194 inches is shown at the weld centerline.

POINT	TEMPERATURE DEGREE S F.	ELASTIC MODULUS E, PSI	THERMAL COEFF. α F	YIELD STRESS T_Y, PSI
1	200	29.0×10^6	6.5×10^{-6}	13.8×10^4
2	800	26.0×10^6	7.7×10^{-6}	11.0×10^4
3	1400	5.0×10^6	8.175×10^{-6}	25.5×10^3
4	1600	4.0×10^6	7.05×10^{-6}	11.2×10^3
5	2500	4.0×10^4	7.45×10^{-6}	1.12×10^3
6	5000	4.0×10^4	7.5×10^{-6}	1.12×10^3

MATERIAL PROPERTIES
SHRINKAGE FORCE METHOD

SOURCE: REFERENCE 5

TABLE II-C-1

RUN "TIME"	TEMP °F	THERMAL CYCLE	
0.0	200°	Layer 1 heatup	
1.0	500°		
2.0	800°		
3.0	1000°		
4.0	1200°		
5.0	1400°		
6.0	1600°		
7.0	1800°		
8.0	2000°		
9.0	2250°		
10.0	2500°F	End	Activate Layer 1
11.0	2250°		
12.0	2000°		
13.0	1800°		
14.0	1600°		
15.0	1400°		
16.0	1200°		
17.0	1000°		
18.0	800°		
19.0	500°		
20.0	200°	End	
21.0	500°	Layer 2 heatup	
22.0	800°		
23.0	1000°		
24.0	1200°		
25.0	1400°		
26.0	1600°		
27.0	1800°		
28.0	2000°		
29.0	2250°		
30.0	2500°	End	Activate Layer 2
31.0	2250°	Layer 2 cooldown	
32.0	2000°		
33.0	1800°		
34.0	1600°		
35.0	1400°		
36.0	1200°		
37.0	1000°		
38.0	800°		
39.0	500°		
40.0	200°	End	

TABLE II-C-2

NONSAP RUN "TIMES"

RUN "TIME"	TEMP. °F	THERMAL CYCLE	
41.0	500°	Layer 3 heatup	
42.0	800°		
43.0	100°		
44.0	1200°		
45.0	1400°		
46.0	1600°		
47.0	1800°		
48.0	2000°		
49.0	2250°		
50.0	2500°	End	Activate Layer
51.0	2250°	Layer 3 cooldown	3
52.0	2000°		
53.0	1800°		
54.0	1600°		
55.0	1400°		
56.0	1200°		
57.0	1000°		
58.0	800°		
59.0	500°		
60.0	200°	End	
		End of Analysis	

TABLE II-C-2
(CONTINUED)

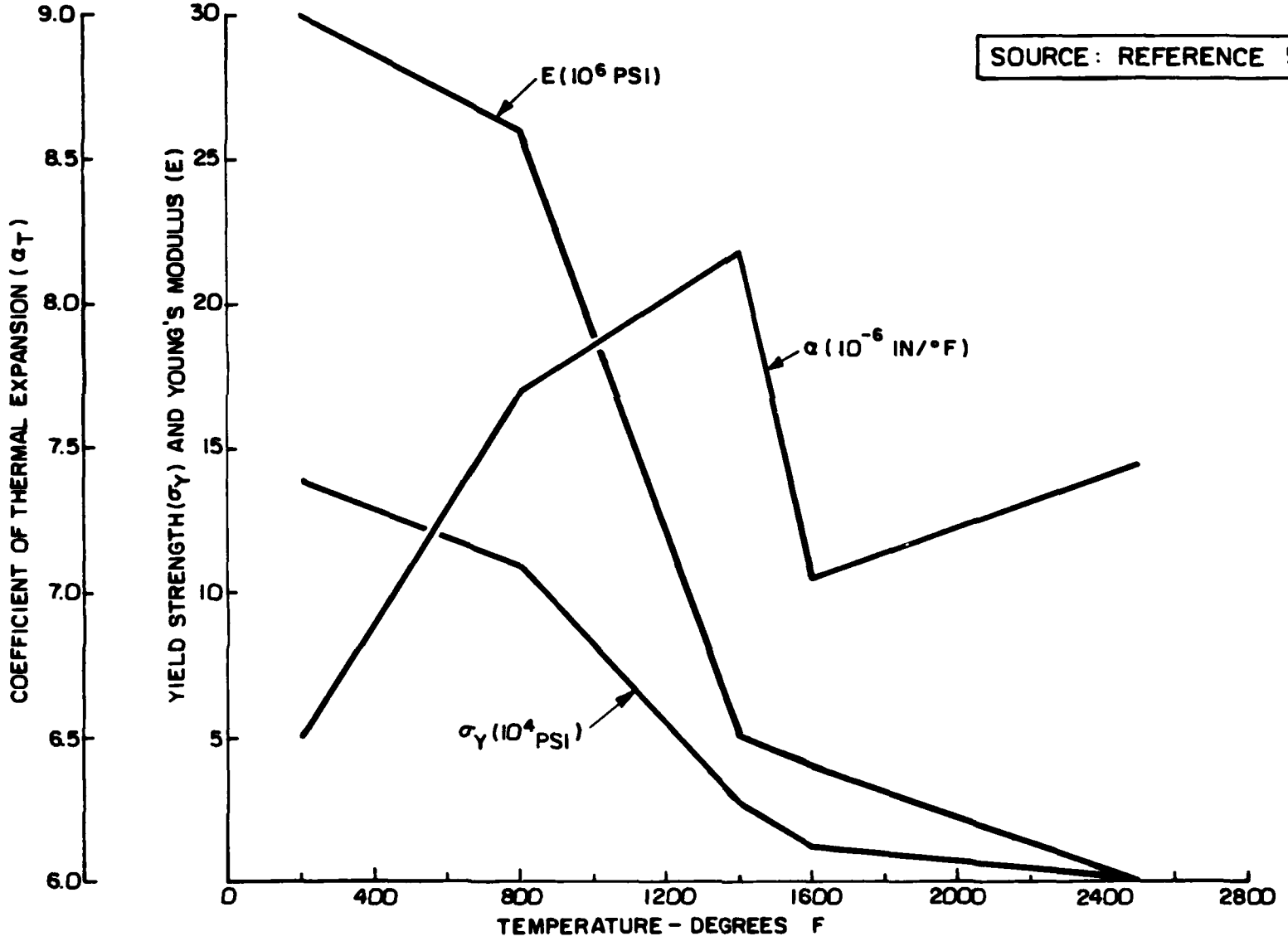
SOURCE: REFERENCE 5
E (10⁶ PSI)
α (10⁻⁶ IN/°F)
σY (10⁴ PSI)
COEFFICIENT OF THERMAL EXPANSION (αT)
YIELD STRENGTH (σY) AND YOUNG'S MODULUS (E)
TEMPERATURE - DEGREES F
9.0
8.5
8.0
7.5
7.0
6.5
6.0
30
25
20
15
10
5
0
400
800
1200
1600
2000
2400
2800

FIGURE II-C-1

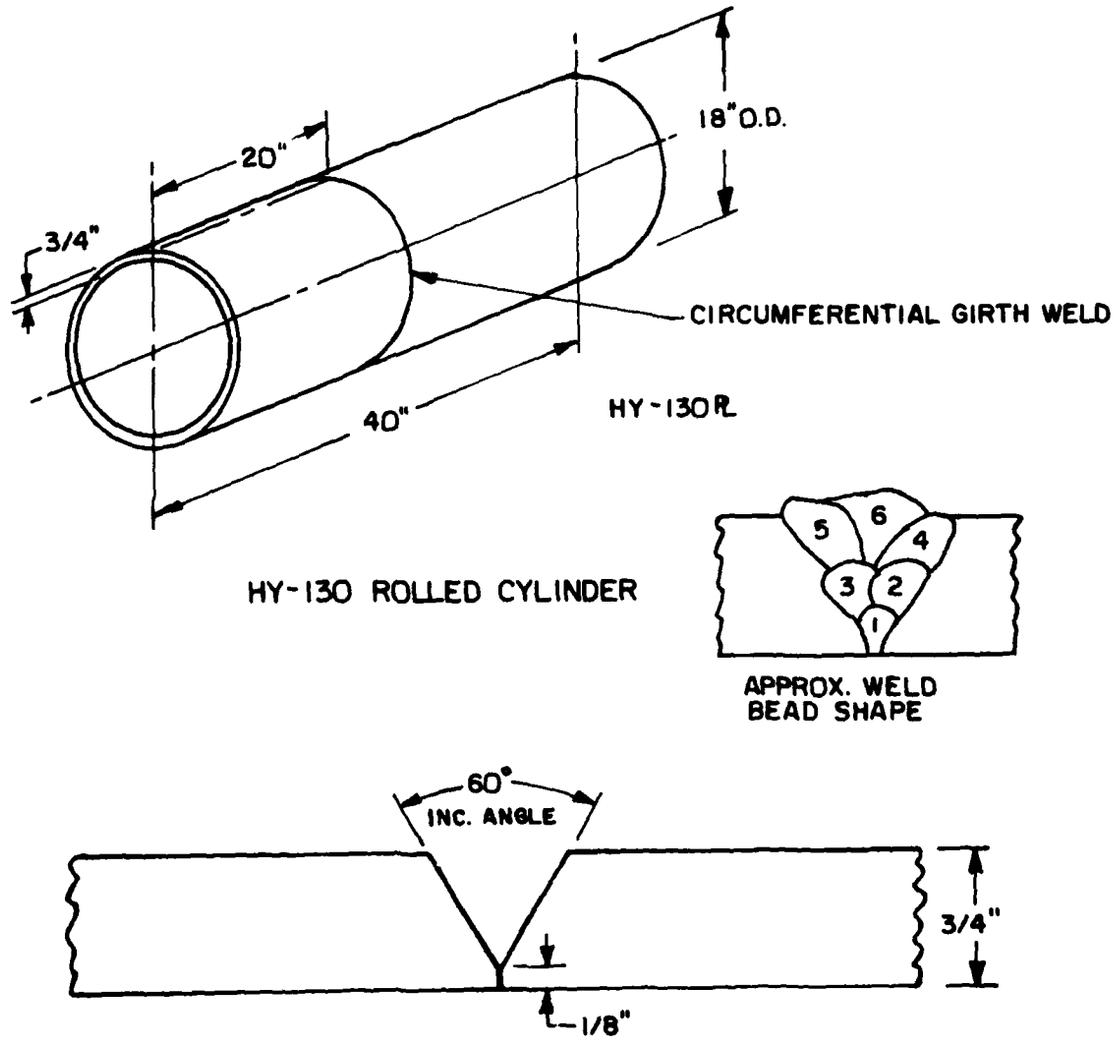

WELD JOINT GEOMETRY FOR HY-130 CYLINDER

FIGURE II-C-2

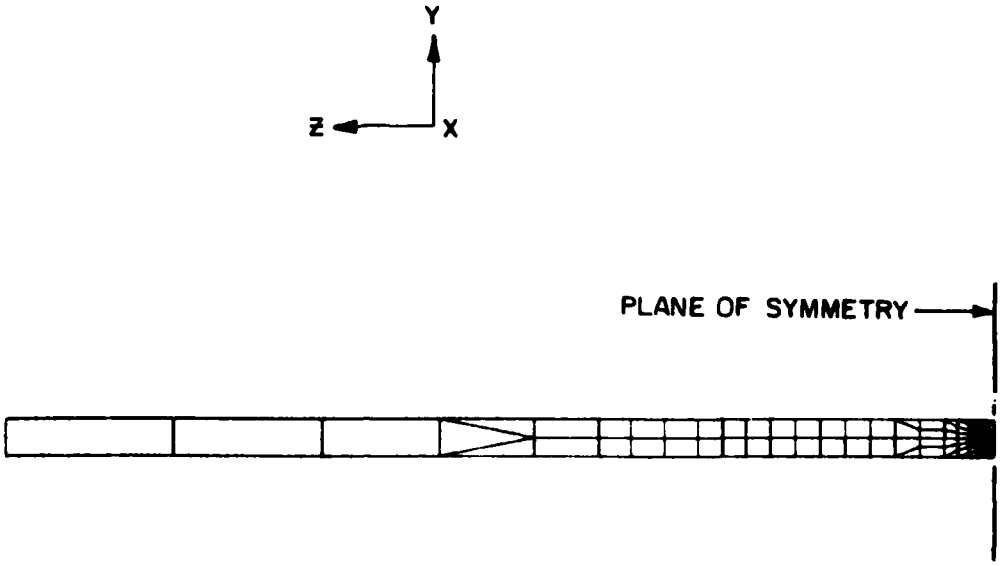

NONSAP MATH MODEL

FIGURE II-C-3

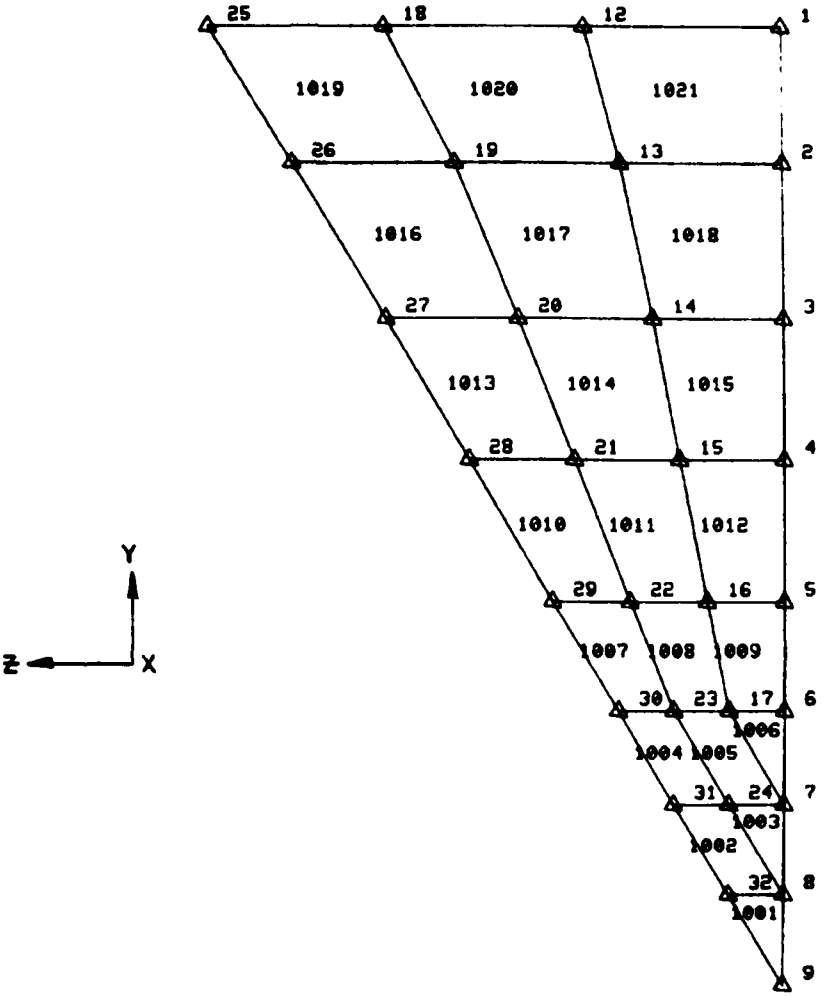

NONSAP MATH MODEL

FIGURE II-C-4

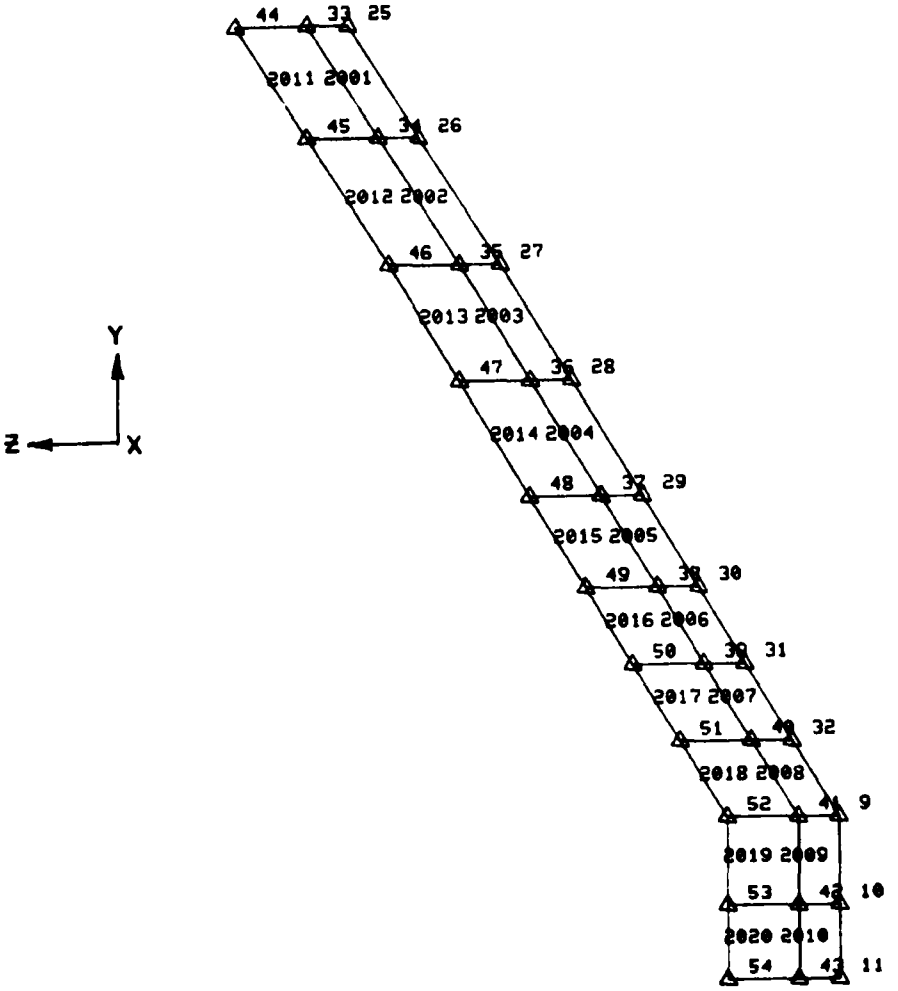

NONSAP MATH MODEL

FIGURE II - C - 5

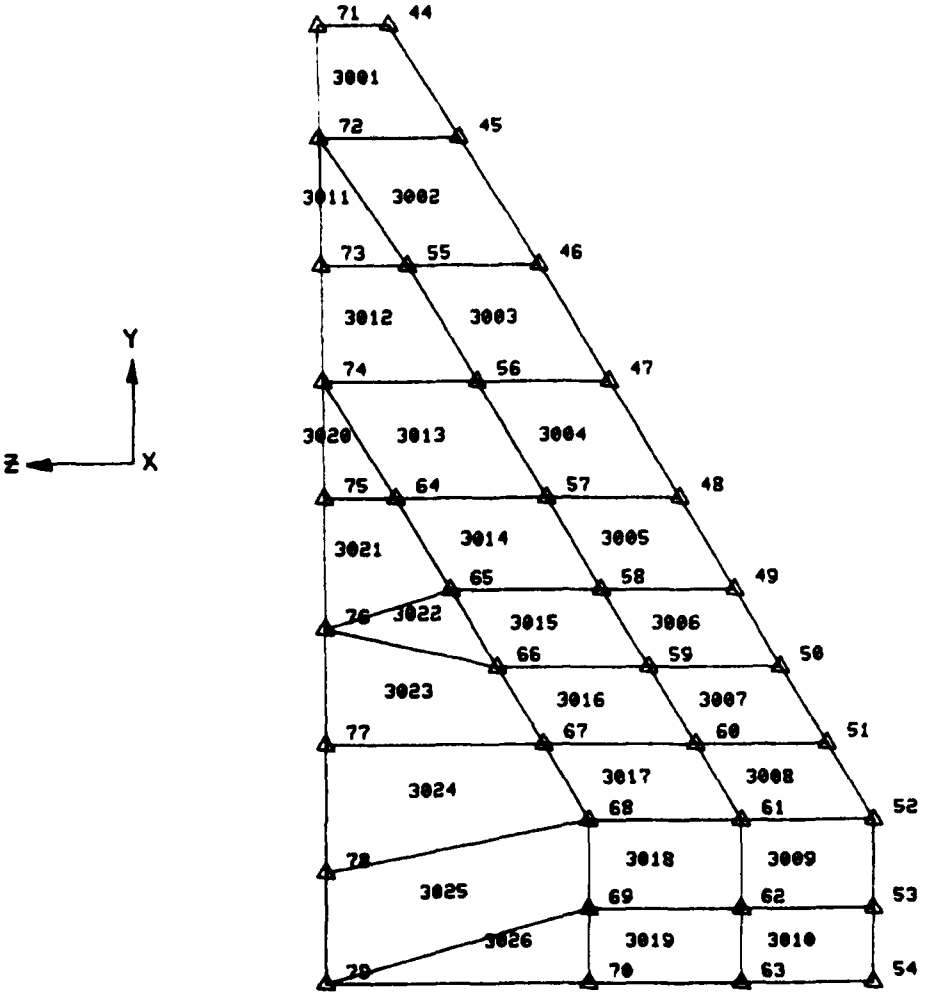

NONSAP MATH MODEL

FIGURE II-C-6

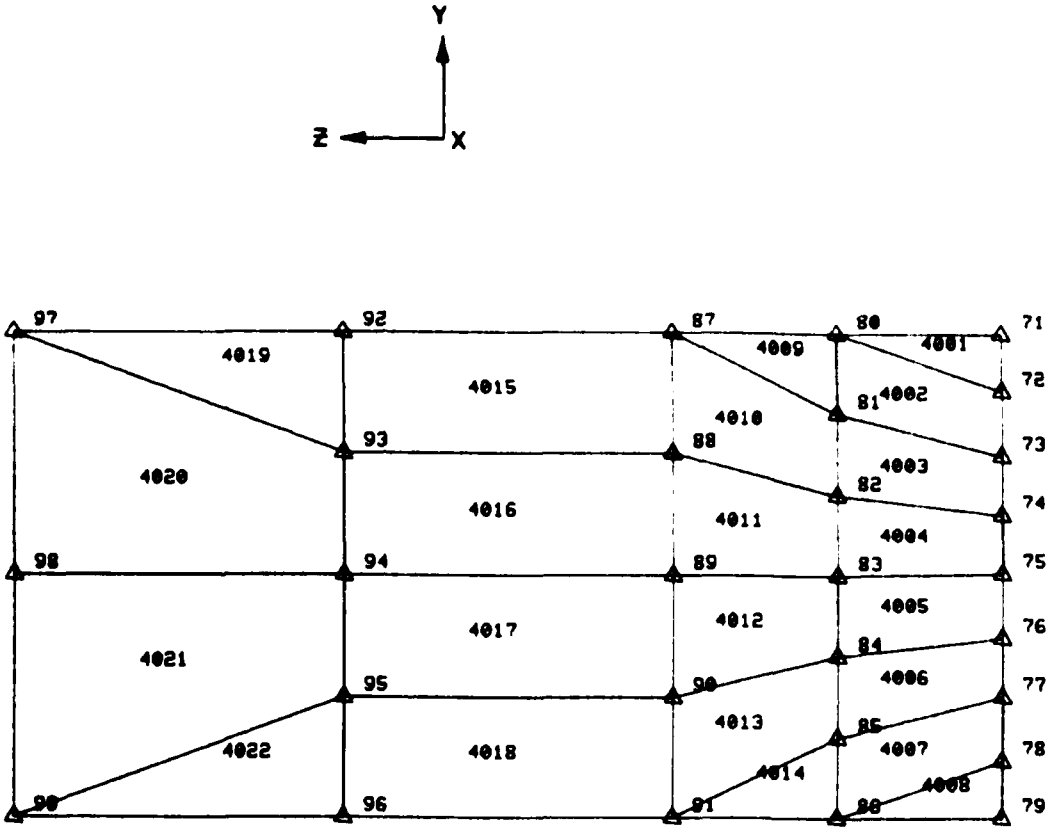

NONSAP MATH MODEL

FIGURE II-C-7

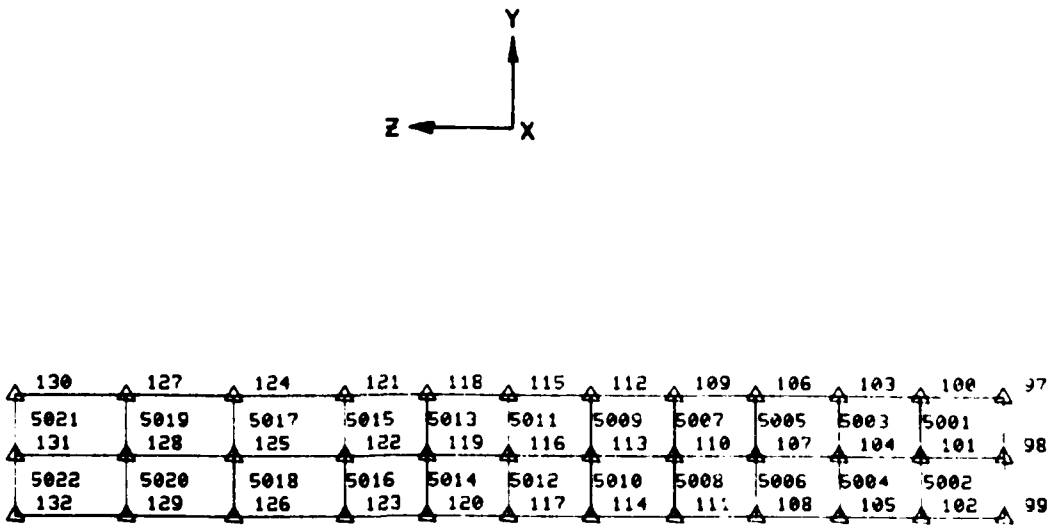

NONSAP MATH MODEL

FIGURE II-C-8

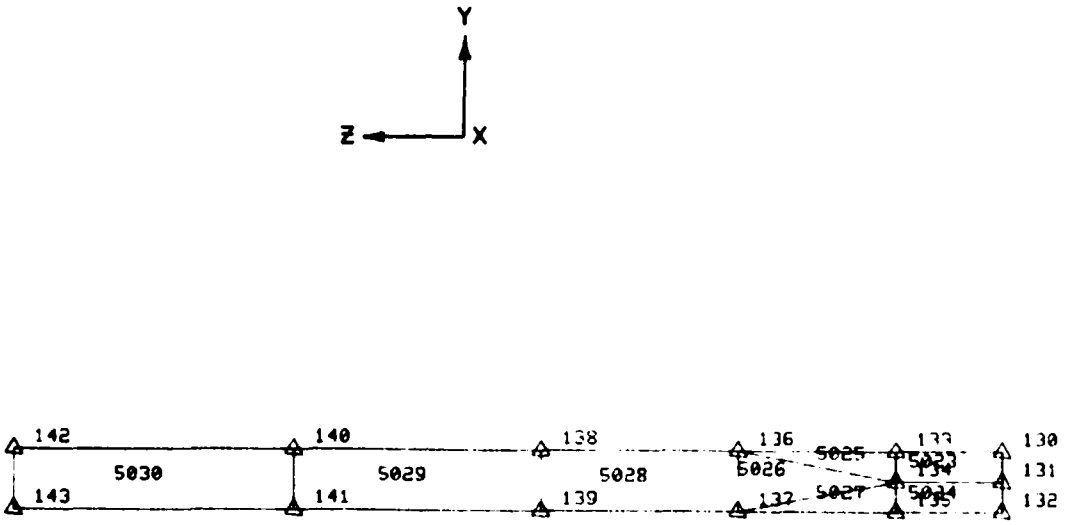

NONSAP MATH MODEL

FIGURE II-C-9

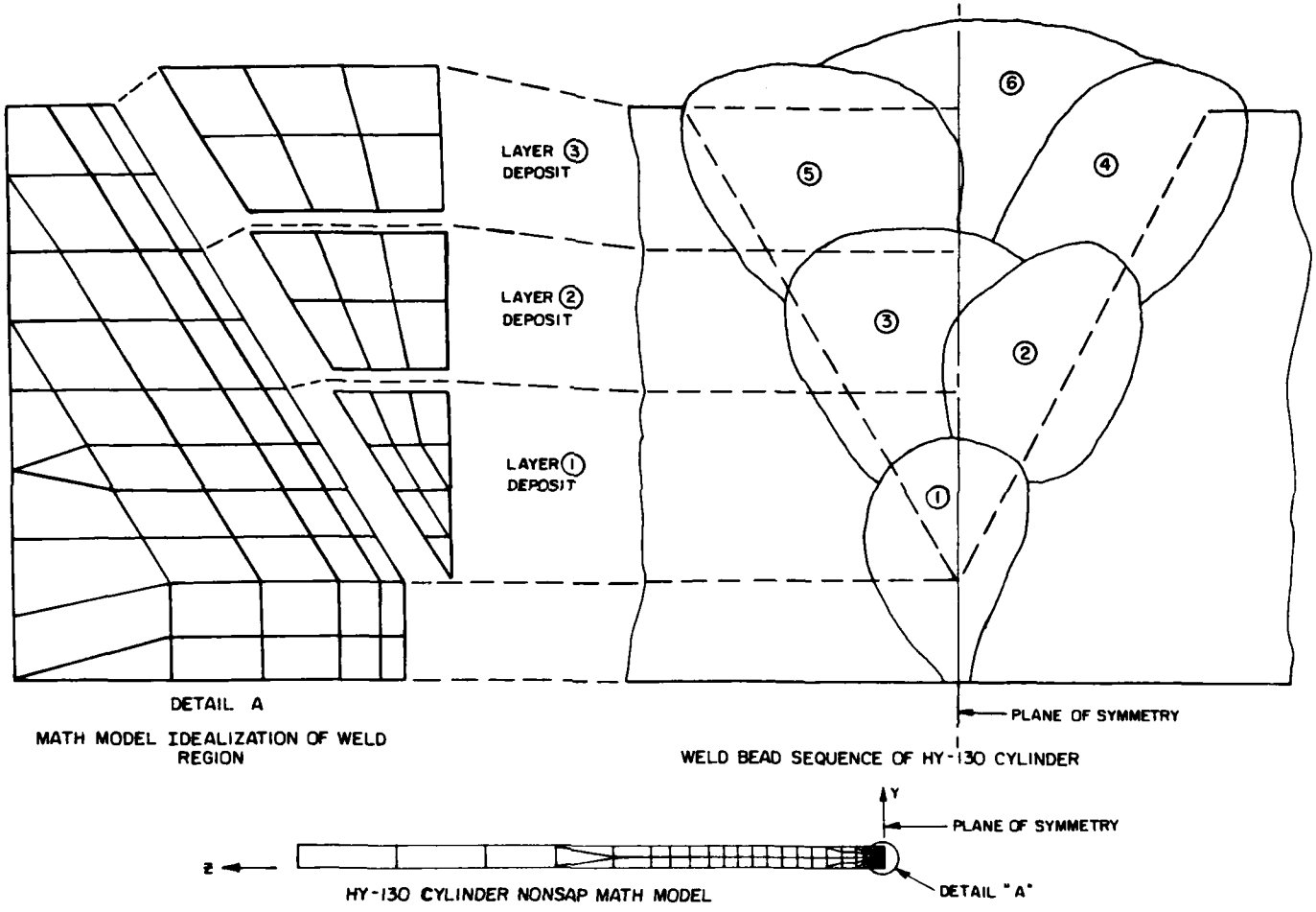

FIGURE II-C-10

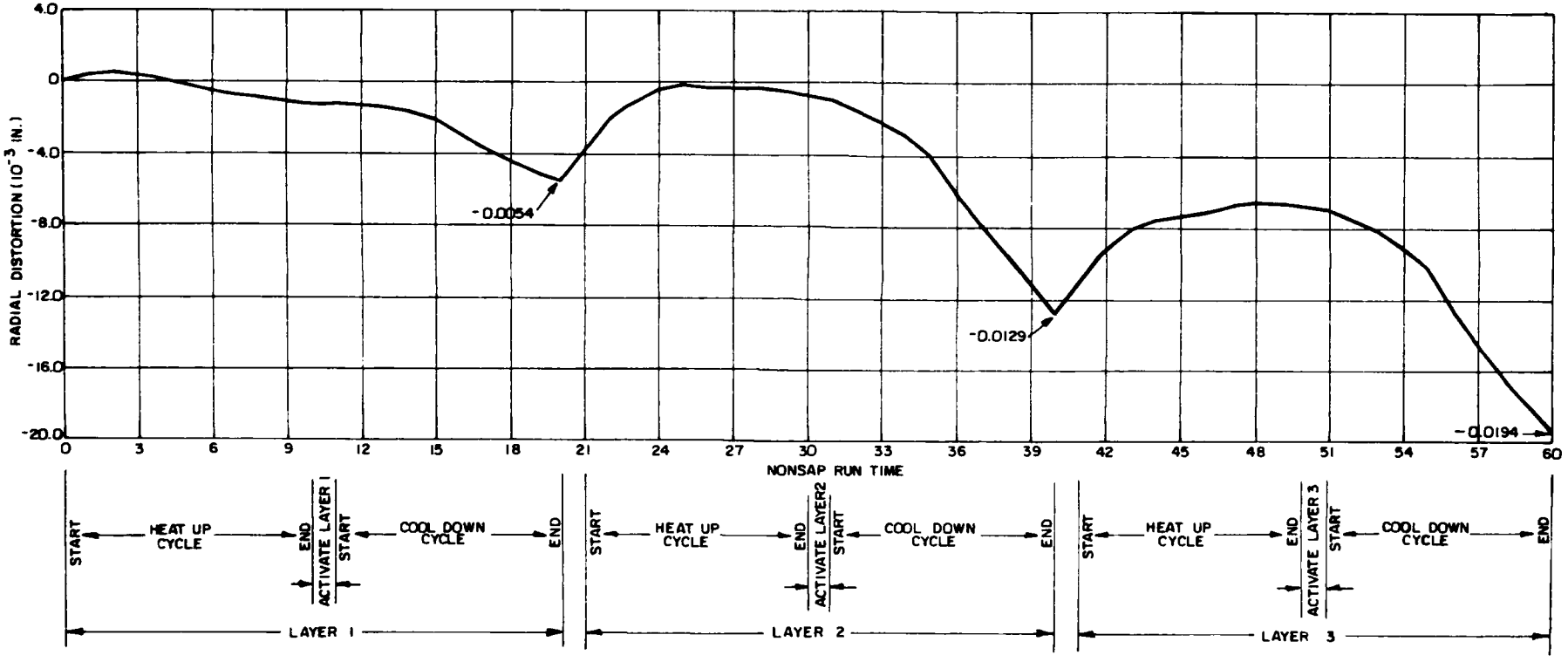

CUMULATIVE RADIAL DISTORTION AT WELD ℄
vs. NONSAP RUN TIME SEQUENCE

FIGURE II-C-11

NOTE: AFTER LAYER 1 COOLDOWN -0.0054
AFTER LAYER 2 COOLDOWN -0.0129
AFTER LAYER 3 COOLDOWN -0.0194

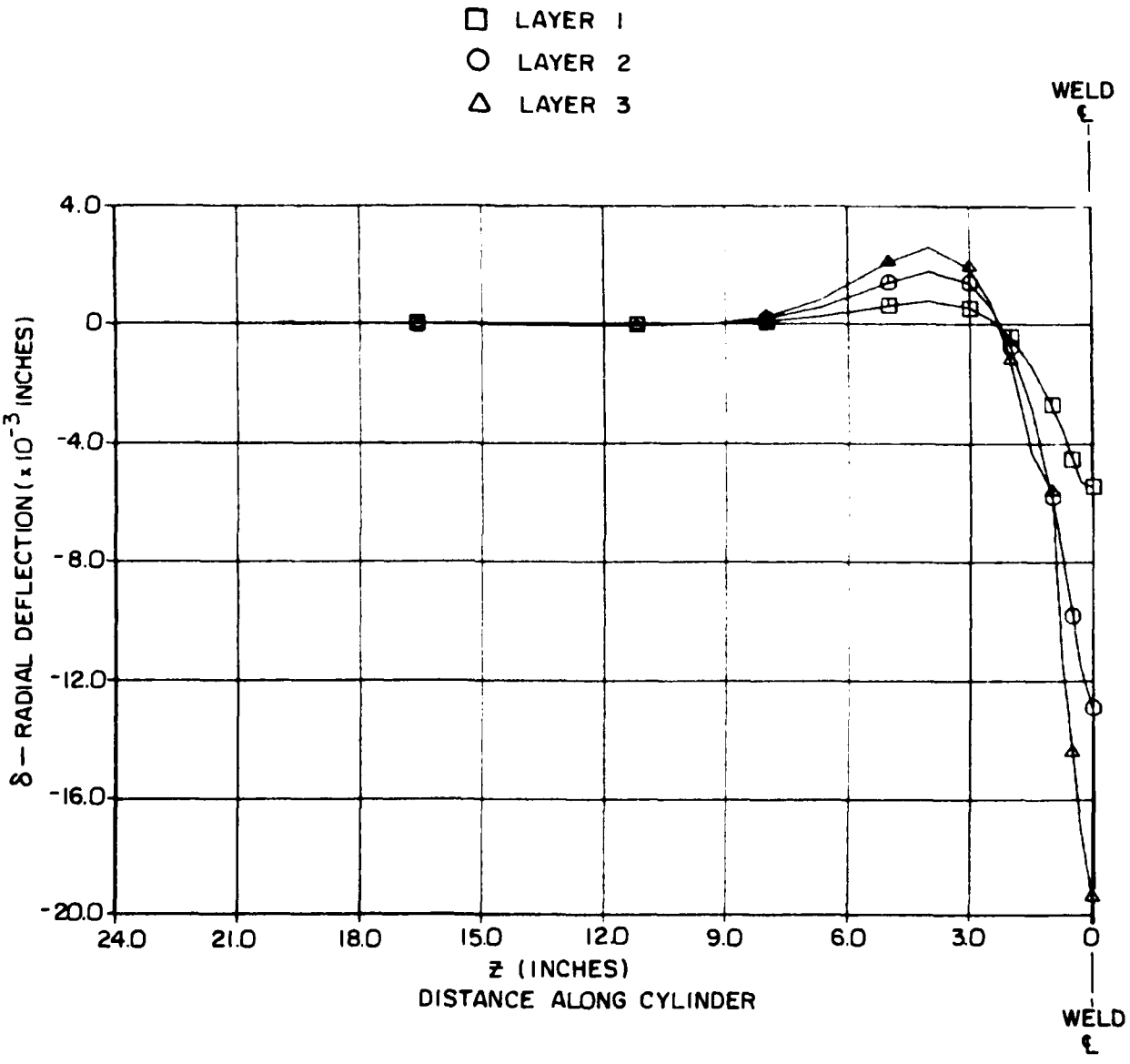

INCREMENTAL LAYER RADIAL DEFLECTIONS
vs. CYLINDER LENGTH

FIGURE II-C-12

III. SHRINKAGE FORCE METHOD ANALYSIS OF SUBMARINE HULL CYLINDER GIRTH WELD

o Background

In 1977, the hull butt between cylinders 20 and 21 of the SSN704 was selected by the Welding Engineering Department for evaluation of a single vee hull butt joint design, with ceramic backing strip on the outside of the hull, and all welding performed from the inside of the hull. The primary objective of the Welding Engineering test was to see if it was possible to minimize, if not completely eliminate back-gouging. Special steps were taken to control the weld prep geometry and to carefully monitor the weld distortion. Since the weld prep geometry and actual welding of the joint was tightly controlled, it provided an excellent opportunity to obtain extensive distortion measurements. These experimental measurements have proven to be an excellent data base for evaluation of analytical methods for predicting weld distortion of hull butt joints. The detailed distortion measurements and a description of the measurement procedure are given in Reference 6.

The original analytical approach, in which the molten metal was assumed to behave elastically, was applied to this problem in 1977, using the BOSOR4 computer code (see Reference 7). The conservativeness of this approach led to an overprediction of final distortion by a factor of approximately 2. In 1978, this joint was re-analyzed using the BOSOR5 code (see Reference 8) to include plastic material behavior of the weld metal. The main difference in this approach is that the weld metal during cooldown is limited to developing a maximum Von-Mises effective stress equal to the specified filler metal yield strength at room temperature. This change provides an upper limit on the maximum force that the cooling, shrinking weld metal can exert on the pieces being welded. The distortion of the elastic-plastic approach was approximately 50 percent of the previous analysis and quite closely approximates the experimental results. See Figure III-1.

Improvement of the analytical approach, the "shrinkage force" method, was undertaken in 1979. The effort concentrated on two areas: one was to gather additional experimental data on the amount of remelt for various welding techniques. The other was to include the effects of remelt in the analytical model. The results of this effort are reported in this section.

o Experimental Results

The extent of base plate melt which occurs during welding had previously been assumed to be 1/8" on each side of the weld joint. This assumption was based on the judgement of welding engineers. This melted base plate was assumed to act with the deposited weld metal, thus increasing the transverse distance across the weld joint by 1/4" in the analytical model of the weld region. Since weld test samples for a number of different weld processes are now available, it was possible to evaluate this assumption quantitatively. The results showed that base plate melt is significantly less than originally assumed - ranging from 1/16" to 1/64", and generally about 1/32" (see Table III-1). This is attributed to the fact that the plates being welded provide a large heat sink to rapidly conduct the welding heat away from the sides of the weld joint, thus minimizing the lateral base plate melt.

The experimental data gathered also shows that the only significant melting which occurs as a result of depositing a weld bead is remelt of previously deposited metal and is directly below the new bead. The ratio of remelted metal to the new metal deposited for various weld processes is shown in Table III-2. A typical macrograph from which this type of data was extracted is pictured in Figure III-4.

LATERAL BASE PLATE MELT (INCH)	WELD PROCESS	HEAT INPUT (KJ/IN)
1/32	SMAW	55
1/32	SAW	55
1/32	GMAW (PULSE)	110

TABLE III-1
LATERAL BASE PLATE MELT
FOR VARIOUS WELD PROCESSES

RATIO OF REMELTED METAL TO NEW WELD METAL DEPOSITED	WELD PROCESS	HEAT INPUT* (KJ/IN)
0.6	GMAW (SPRAY)	55
1.0	SMAW	55
1.0	GMAW (PULSE)	110
1.5	SAW	55

TABLE III-2
REMELTED METAL TO NEWLY DEPOSITED
WELD METAL RATIOS

*Heat input of 55 KJ/in is the current maximum allowed by welding specifications. The 110 KJ/in is considered high heat input and was done for experimental purposes only.

o Analytical Results

In 1979 the SSN704 weld joint was re-analyzed using the BOSOR5 computer code considering elastic-plastic material behavior, 1/32 inch lateral base plate melt, various remelt depths, and a stress relief force system to simulate the effects of re-melt. For treating the re-melt phenomenon in the analytical model; where the weld metal is assumed to be deposited in layers, equations 1, 2, and 3 were derived to calculate membrane and bending forces acting at the mid-plane of the weld segment equivalent to the stresses existing in the metal which is assumed to be remelted. The negative of this force system is applied to the analytical model to simulate the effect of relieving the stresses in the re-melted metal. See Figure III-2.

Equation 1 AXIAL LOAD

$$N = \frac{t_R}{2} (\sigma_{Z1M} + \sigma_{Z2M})$$

Equation 2 MOMENT LOAD

$$M = \sigma_{Z1M} \left[t_R\left(\frac{Z_1}{2} + \frac{t_R}{6}\right)\right] + \sigma_{Z2M} \left[t_R\left(\frac{Z_1}{2} + \frac{t_R}{3}\right)\right]$$

Equation 3 RADIAL LOAD

$$H = C1 \cdot \frac{t_R}{4R} \cdot (\sigma_{Z1C} + \sigma_{Z2C}) - C2 \cdot \frac{t_R}{2R} \cdot \left[\sigma_{Z1C} \cdot \left(\frac{Z_1}{2} + \frac{t_R}{6}\right) + \sigma_{Z2C} \cdot \left(\frac{Z_1}{2} + \frac{t_R}{3}\right)\right]$$

See Figure III-2 for definition of terms.

The results of the BOSOR5 elastic-plastic analyses for 1/2, 1, and 2 layer assumptions of remelt are shown in Figure III-3 together with the measured distortion curve. Distortions for various remelt depths were predicted in order to determine the effect of remelt depth on distortion. The 1/2 layer remelt condition is the closest approximation (about 10% error) of the SSN704 data which is to be expected since that joint was welded with the GMAW process.

o Summary of Results

1. For the SSN704 circumferential hull butt, the most recent analytical method (BOSOR5 elastic-plastic including 1/32" lateral base plate melt, single bevel, $\Delta T = 1300^{\circ}F$ and 1/2 layer remelt) yielded a distortion prediction within 10% of the measured distortion. This was not as accurate as the distortion predicted by the 1978 BOSOR5 elastic-plastic analysis without remelt which was within 5% of the measured distortion. However, both predictions are considered within engineering accuracy.

2. Predicted distortion when remelt is considered via the applied stress relief force system increases as the depth of remelt increases. This is just the opposite of what one would expect. Greater remelt should cause more stress relief and less distortion.

3. The most recent analytical method which includes stress relief is fairly sensitive for changes in remelt penetration into the previously deposited weld metal. As the remelt depth was increased from 1/2 to 1 to 2 layers the predicted distortion increased from .117" to .149" to .182" or about 55% over the range considered.

4. Based on weld test sample evaluation, a base plate melt of 1/32" on each side of the weld joint is the correct value for use in the analytical model.

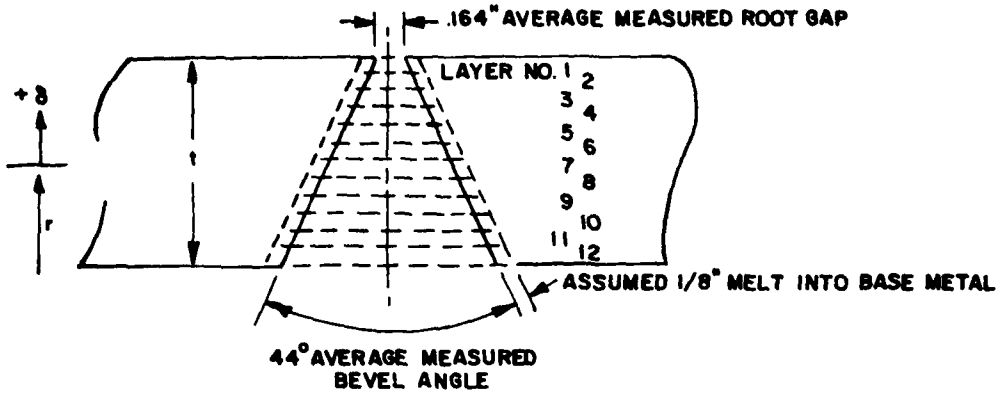
.164" AVERAGE MEASURED ROOT GAP
LAYER NO. 1
2
3
4
5
6
7
8
9
10
11
12
+δ
t
r
ASSUMED 1/8" MELT INTO BASE METAL
44° AVERAGE MEASURED
BEVEL ANGLE

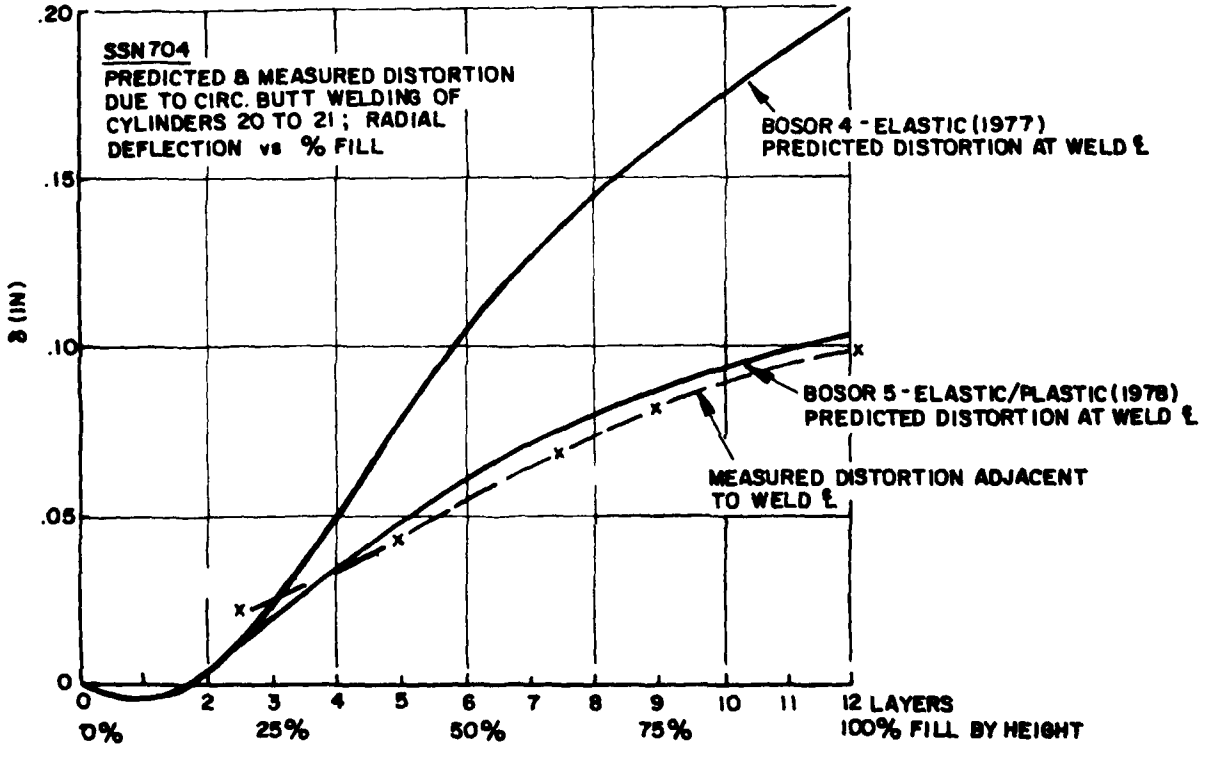
SSN 704
PREDICTED & MEASURED DISTORTION
DUE TO CIRC. BUTT WELDING OF
CYLINDERS 20 TO 21; RADIAL
DEFLECTION vs % FILL
BOSOR 4 - ELASTIC (1977)
PREDICTED DISTORTION AT WELD ℄
BOSOR 5 - ELASTIC/PLASTIC (1978)
PREDICTED DISTORTION AT WELD ℄
MEASURED DISTORTION ADJACENT
TO WELD ℄
δ (IN)
.20
.15
.10
.05
0
0
2
3
4
5
6
7
8
9
10
11
12 LAYERS
0%
25%
50%
75%
100% FILL BY HEIGHT

FIGURE III - 1

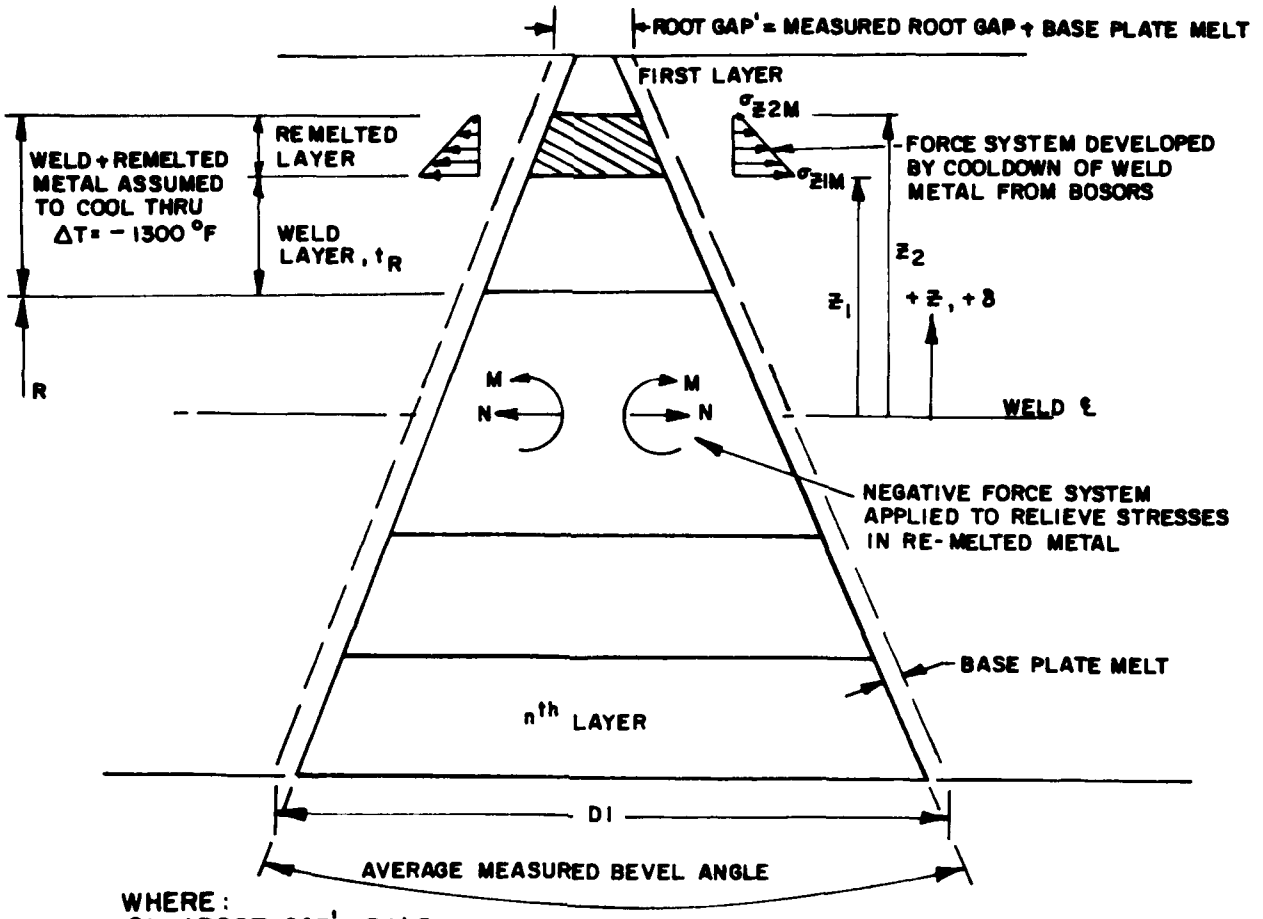

WHERE:

$C1 = (ROOT\ GAP' + DI)\,2$

$C2 = \left[TANGENT\ (BEVEL\ ANGLE/2)\right] \times 2$

H = RADIAL LINE LOAD

M = LINE MOMENT LOAD

N = AXIAL LINE LOAD

R = MID SURFACE RADIUS OF SHELL

t_R = THICKNESS OF WELD LAYER

z_1 = RADIAL DISTANCE FROM WELD ℄ TO INNER SURFACE OF REMELTED LAYER

z_2 = RADIAL DISTANCE FROM WELD ℄ TO OUTER SURFACE OF REMELTED LAYER

σ_{Z1C} = CIRCUMFERENTIAL STRESS AT DISTANCE z_1

σ_{z1M} = MERIDIONAL STRESS AT DISTANCE z_1

σ_{z2C} = CIRCUMFERENTIAL STRESS AT DISTANCE z_2

σ_{z2M} = MERIDIONAL STRESS AT DISTANCE z_2

FIGURE III - 2

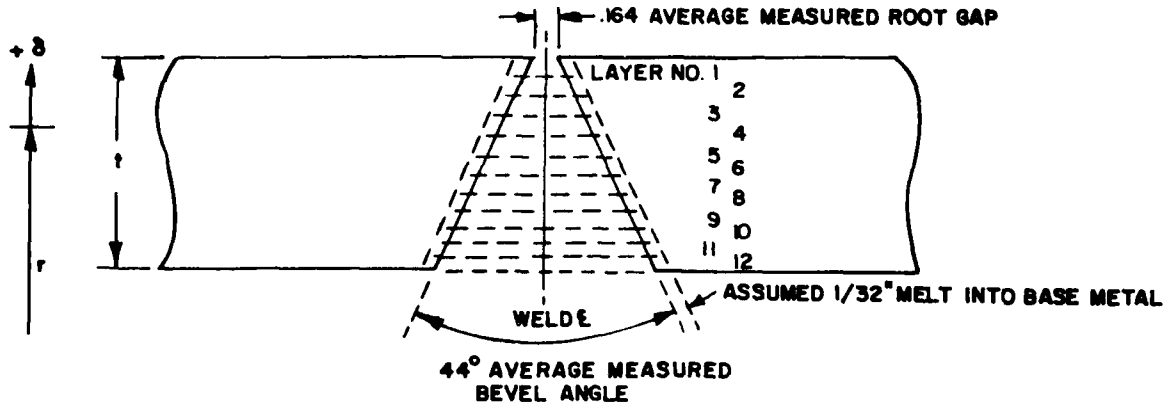
.164 AVERAGE MEASURED ROOT GAP
+δ
t
r
LAYER NO. 1
2
3
4
5
6
7
8
9
10
11
12
ASSUMED 1/32" MELT INTO BASE METAL
WELD ℄
44° AVERAGE MEASURED
BEVEL ANGLE

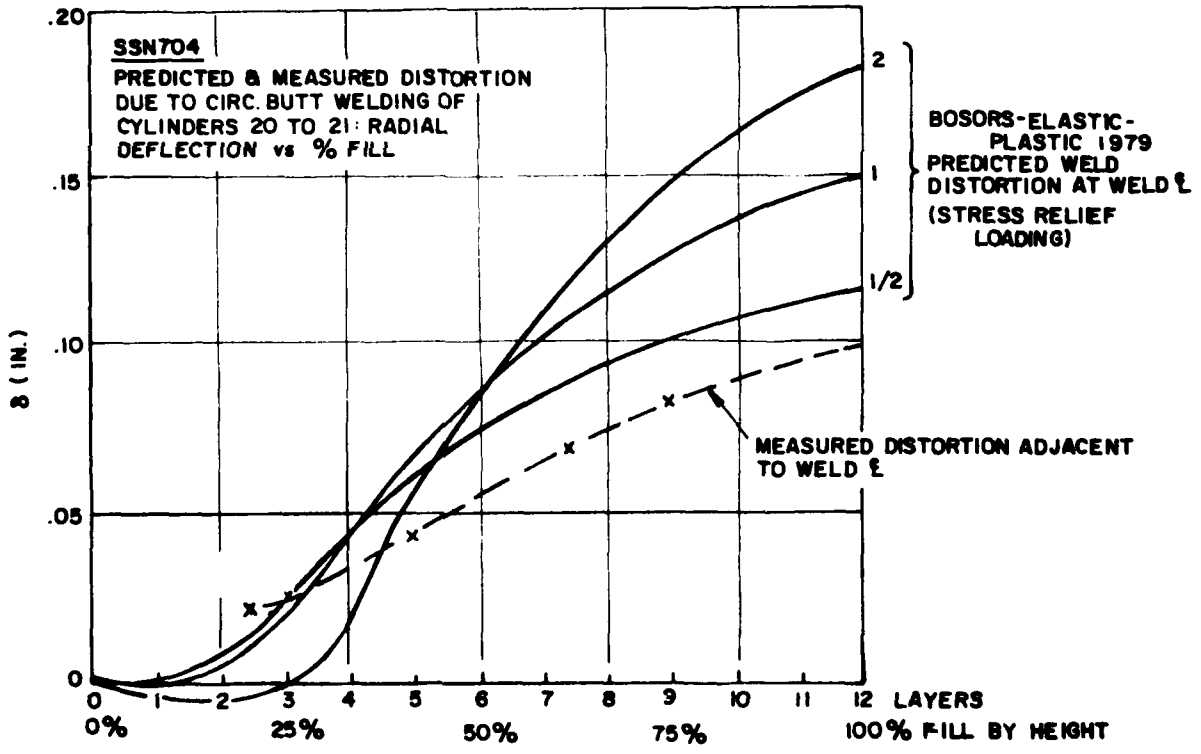
SSN704
PREDICTED & MEASURED DISTORTION
DUE TO CIRC. BUTT WELDING OF
CYLINDERS 20 TO 21: RADIAL
DEFLECTION vs % FILL
.20
.15
.10
.05
0
δ (IN.)
2
1
1/2
BOSORS-ELASTIC-
PLASTIC 1979
PREDICTED WELD
DISTORTION AT WELD ℄
(STRESS RELIEF
LOADING)
MEASURED DISTORTION ADJACENT
TO WELD ℄
0 1 2 3 4 5 6 7 8 9 10 11 12 LAYERS
0%
25%
50%
75%
100% FILL BY HEIGHT

FIGURE III - 3

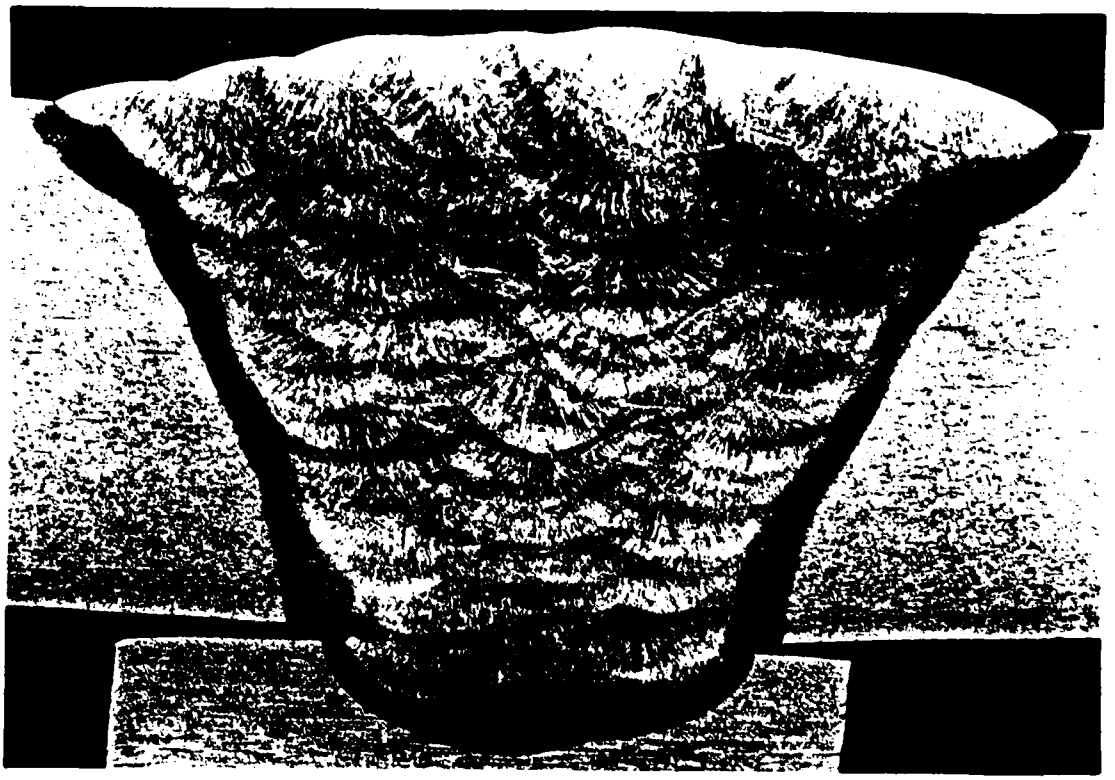

WELD BEAD MACROGRAPH
OF SAW WELD TEST
PLATE WT 595
(≈3 x MAGNIFICATION)

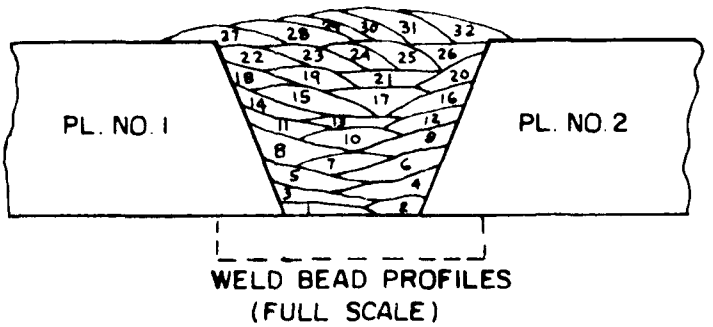

FIGURE III - 4

IV CONCLUSIONS AND RECOMMENDATIONS

o Heat Transfer Analysis of HY-130 Cylinder Girth Weld

The comparison of the predicted and experimental temperatures for the first weld pass show a large deviation, up to 200°F, for a surface node located 1.0 inches away from the weld pool. The amount of deviation decreases for nodes further away from the pool. The probable reason for this discrepancy is the presently uncertain value of the specific heat of the weld metal in the liquid state, as explained in Section II-A-3. This hypothesis may be proven by a two-step approach, as follows.

1) Perform additional computations utilizing trial values of the liquid specific heat until the predicted and experimental temperatures agree. A resultant specific heat of the order of five or less times the solid state specific heat would indicate the likelihood of the hypothesis. An extremely high specific heat would negate the hypothesis.

2) Presuming that (1) above indicates a likelihood, determine the specific heat and other thermodynamic properties of the liquid state experimentally.

- Shrinkage Force Method of Analysis of HY-130 Cylinder Girth Weld via NONSAP

The results of the subject analysis look quite good by inspection. Distortion during heat-up and cooldown cycles follows a logical pattern. However, when comparing to the experimental results, it was found that for the first layer of weld the predicted distortion (.0054" inward) was in the opposite direction of both the measured and calculated values reported in Reference 3. Interestingly, an examination of the residual strain magnitudes measured in the test seem to support a distorted shape as indicated in Figure II-C-12 of this report. Also, the transient temperature distribution measured in the test shows that the HY-130 cylinder was not allowed to cool back down to the 200°F preheat temperature where predicted and experimental distortions could be compared. The only correlation with test data is the initial outward distortion shown in Figure II-C-11 when the weld boundary nodes are in the first heat-up cycle.

A trip was made to MIT to obtain any additional test data that might help resolve the above discrepancies. It was learned that no distortion or temperature test data was available for welding after the first bead. An examination of strips cut out of the HY-130 cylinder in way of the girth weld showed that:

1. The first weld bead did not penetrate through the bevel land.

2. The mating bevel lands were touching (after welding).

Both of these tend to support the Electric Boat Division boundary conditions and model at the plane of symmetry (weld centerline). However, if the bevel lands were not clamped tight together (i.e., slightly separated) during first pass welding, an outward deflection as measured could be expected. Another test similar to that performed at MIT is required to resolve the discrepancies. However, to obtain maximum utility from the experimental data, this next test must be tightly controlled and well documented. Transient and final (cooled down) measurements of temperature, distortion and stress are required for every weld bead and/or weld layer.

o Submarine Hull Cylinder Girth Weld Analysis

The results obtained when applying the Shrinkage Force Method to the SSN704 hull butt raised two important questions:

1. Why did the distortion predictions incorporating remelt stress relief loadings increase with remelt depth?

2. Which variation of the Shrinkage Force Method in the axisymmetric case will accurately, cost-effectively, and consistently predict weld distortions.

o Recommendations

The following tasks are recommended for future investigation:

1. In the heat transfer problem perform additional computations varying the liquid weld metal specific heat until predicted and experimental temperatures agree in order to prove or disprove the hypothesis that the probable reason for the discrepancy between the predicted and measured temperatures is the uncertain value of liquid specific heat.

2. Experimentally determine the specific heat and possibly other key thermodynamic properties of liquid weld metal.

3. Conduct a sensitivity study of the temperature-dependent characteristics of the mechanical (structural) properties of the weld filler material. This will identify the structural parameter (or parameters) that are key properties; and, therefore identify those areas where high-temperature property testing should be concentrated.

4. Future effort should also be devoted to the development or acquisition of a computer program for the prediction of the three-dimensional temperature distribution in the weld pool and base metal including the effect of the movement of the weld rod. It is potentially possible that transient temperature distribution can be obtained from the equivalent steady state solution of the problem cast so that the thermal field stays in a fixed position relative to the weld rod.

5. Perform a tightly controlled and well documented test similar to that reported in Reference 5 measuring distortions, temperatures and induced strains for each weld bead or layer.

6. Obtain additional hull distortion measurements in way of submarine circumferential butt weld to expand and increase the confidence level in the experimental data base. This type of data is invaluable in analytical correlation efforts.

7. Apply the various formulations of the Shrinkage Force Method to the submarine hull butts measured in 6. above in order to determine which formulation is the most accurate, cost-effective and consistent approach.

V. REFERENCES

1. Cacciatore, P. J., "Analytical Modeling of Heat Flow and Structural Distortion in Ship Structures Produced by Welding", Technical Report No. 1 for the Office of Naval Research under Contract No. N00014-76-C-0808, October 1977.

2. Cacciatore, P. J. and Morante, R., "Analytical Modelling of Structural Distortion in Ship Structures Produced by Welding", Technical Report No. 2, Office of Naval Research Contract No. N00014-76-C-0808, December 1979.

3. Masubuchi, K. and Papazoglou, V., "Study of Residual Stresses and Distortion in Structural Weldments in High-Strength Steels", Second Progress Report of Contract N00014-75-C-0469, Office of Naval Research, August 31, 1979.

4. Wilson, E. L. and Nickell, R. E., "Application of the Finite Element Method to Heat Conduction Analysis", Nuclear Engineering and Design, Vol. 4, pp. 276-286, 1966.

5. Eldridge, E. A. and Deem, H. W., "Report on the Physical Properties of Metals and Alloys from Cryogenic to Elevated Temperatures", ASTM Special Technical Publication 296, 1961.

6. Morante, R. J., "Development of Weld Distortion/Residual Stress Prediction Methods: Year End Progress Report", EBDiv. Report No. ERR-EB78-005, 1978.

7. Bushnell, D., "Stress, Stability, and Vibration of Complex Branched Shells of Revolution: Analysis and User's Manual for BOSOR4", Lockheed Missiles and Space Co. Report No. LMSC-D243605, 1971.

8. Bushnell, D., "BOSOR5 - A Computer Program for Buckling of Elastic-Plastic Complex Shells of Revolution Including Large Deflections and Creep - Vol. 1: User's Manual, Input Data", Lockheed Missiles and Space Co. Report No. LMSC-D407166, 1974.

UNCLASSIFIED

SECURITY CLASSIFICATION OF THIS PAGE (When Data Entered)

REPORT DOCUMENTATION PAGE		READ INSTRUCTIONS BEFORE COMPLETING FORM
1. REPORT NUMBER U443-80-058	2. GOVT ACCESSION NO. AD-A093 429	3. RECIPIENT'S CATALOG NUMBER
4. TITLE (and Subtitle) Analytical Modelling of Structural Distortion in Ship Structures Produced by Welding		5. TYPE OF REPORT & PERIOD COVERED Technical Report July 1978-July 1980 6. PERFORMING ORG. REPORT NUMBER
7. AUTHOR(s) M. Bartek F. Kocon N. D. Osella		8. CONTRACT OR GRANT NUMBER(s) N00014-76-C-0808
9. PERFORMING ORGANIZATION NAME AND ADDRESS General Dynamics Corporation Electric Boat Division Groton, Connecticut		10. PROGRAM ELEMENT, PROJECT, TASK AREA & WORK UNIT NUMBERS NR 031793
11. CONTROLLING OFFICE NAME AND ADDRESS Office of Naval Research Metallurgy Program Arlington, Virginia		12. REPORT DATE November 1980 13. NUMBER OF PAGES 73
14. MONITORING AGENCY NAME & ADDRESS(if different from Controlling Office) Office of Naval Research Metallurgy Program Arlington, Virginia		15. SECURITY CLASS. (of this report) UNCLASSIFIED 15a. DECLASSIFICATION DOWNGRADING SCHEDULE

16. DISTRIBUTION STATEMENT (of this Report)

The distribution of this document is controlled by the controlling agency.

17. DISTRIBUTION STATEMENT (of the abstract entered in Block 20, if different from Report)

18. SUPPLEMENTARY NOTES

19. KEY WORDS (Continue on reverse side if necessary and identify by block number)

Welding, Simulation, Analysis, Heat Flow, Structural Distortion, Experimental Verification

20. ABSTRACT (Continue on reverse side if necessary and identify by block number)

This report describes various analyses of an HY-130 cylinder girth weld. Analyses were performed to predict transient temperature distribution during girth welding, transient thermoplastic distortions using the predicted temperature distribution and thermomechanical distortions by applying the shrinkage force method. Predicted temperatures and distortions are compared to experimental results.

DD FORM 1 JAN 73 1473 EDITION OF 1 NOV 65 IS OBSOLETE
S/N 0102-014-6601

UNCLASSIFIED

SECURITY CLASSIFICATION OF THIS PAGE (When Data Entered)

ABSTRACT (Continued):

This report also describes the analysis of a submarine circumferential, HY-80 hull butt using the shrinkage force method to predict distortions. Analysis results are compared to experimental data.


DAT
FILM